Supplementary Information

A CRISPR-based ultrasensitive assay redefines “undetectable” SARS-CoV-2 antibodies in kidney transplant recipients after COVID-19 vaccination

Yanan Tang,[1,#] Turun Song,[2,#] Lu Gao,[1] Saifu Yin,[2] Min Ma,[2] Yun Tan,[1] Lijuan Wu,[3] Tao Lin,[2,*] and Feng Li[1,4,*]

Table of Contents

S1. UCAD probe design and optimization

Table S1: DNA sequences and modifications

Name	Sequence (5'→3')
UCAD	
TS Probe	TTC CTC ACC ATG TCT GAG GTA CTC CTT AAA GGT CGA GCT GGA C
NTS Probe	TTG TTG AGG TAA CCA ACT ATT TGT TAC TGT TGC TTG TGG CCG TTT ACG TCG CCG TCC AG
RPA F-primer	TTG TTG AGG TAA CCA ACT ATT TGT TAC TGT T
RPA R-primer	TTC CTC ACC ATG TCT GAG GTA CTC CTT A
dsDNA barcode (sense strand)	TTC CTC ACC ATG TCT GAG GTA CTC CTT AAA GGT CGA GCT GGA CGG CGA CGT AAA CGG CCA CAA GCA ACA GTA ACA AAT AGT TGG TTA CCT CAA CAA
dsDNA barcode (anti-sense strand)	TTG TTG AGG TAA CCA ACT ATT TGT TAC TGT TGC TTG TGG CCG TTT ACG TCG CCG TCC AGC TCG ACC TTT AAG GAG TAC CTC AGA CAT GGT GAG GAA
CRISPR-Cas12a	
crRNA	UUA UUU CUA CUC UUG UAG AUC GUC GCC GUC CAG CUC GAC C
Reporter for fluorescence readout	FAM-TTATT-BHQ-1
Reporter for lateral flow readout	FAM-TTATT-Digoxin

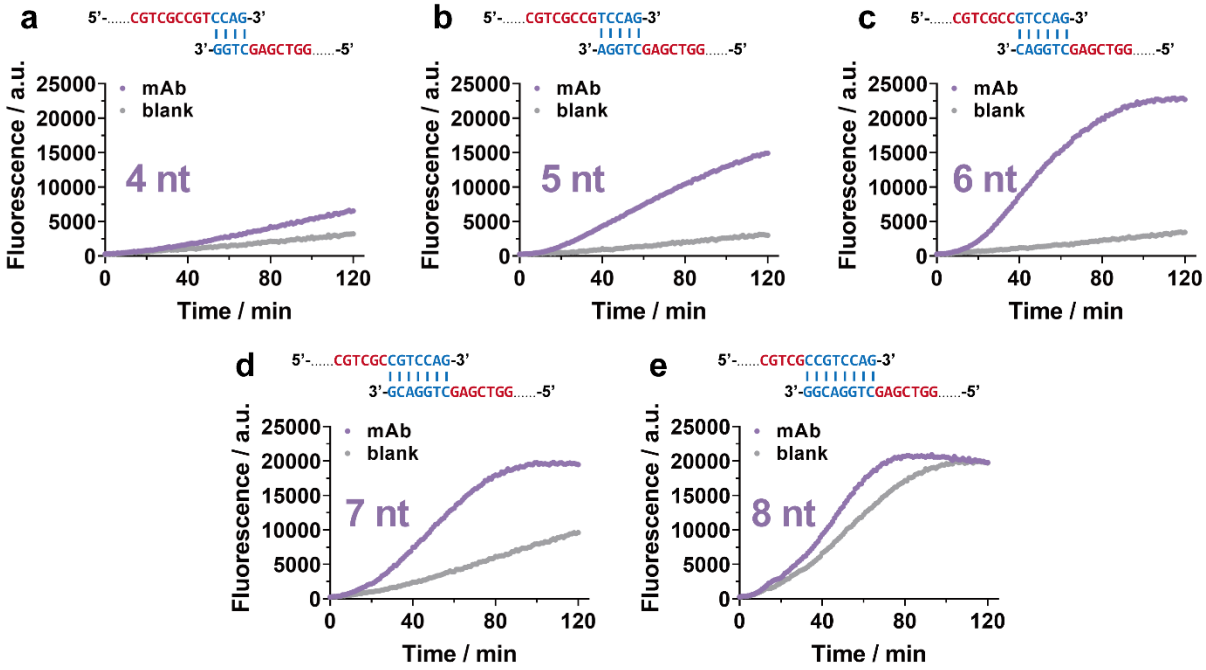

Figure S1 | Optimization of probe design. Optimization of the length of the complementary domain of the TS and NTS probes from 4 nt to 8 nt in detecting anti-RBD mAb by UCAD. Because short complementary domains of the TS and NTS probes (4 nt and 5 nt) produce low fluorescence signal due to insufficient hybridization and probes with long complementary domains (7 nt and 8 nt) produce high fluorescence background due to target-independent hybridization, an optimal length of the complementary domain was found to be 6 nt. [mAb]= 100 fM, [TS probe] = 10 pM, [NTS probe] = 10 pM, [dNTPs]= 40 μM, [Cas12a] = 40 nM, [crRNA] = 40 nM, [Reporter] = 40 nM.

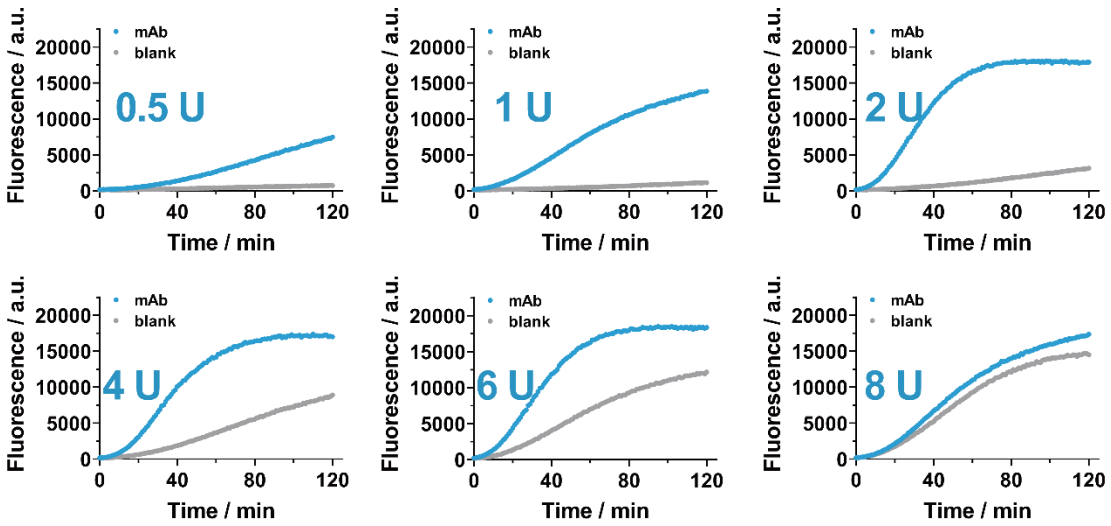

Figure S2 | Optimization of T4 polymerase. Optimization of T4 polymerase from 0.5 U to 8 U per reaction in detecting anti-RBD mAb by UCAD. Based on the maximal differences between signal and background, an optimal concentration of T4 polymerase was found to be 2U per reaction. [mAb]= 100 fM, [TS probe] = 10 pM, [NTS probe] = 10 pM, [dNTPs]= 40 μM, [Cas12a] = 40 nM, [crRNA] = 40 nM, [Reporter] = 40 nM.

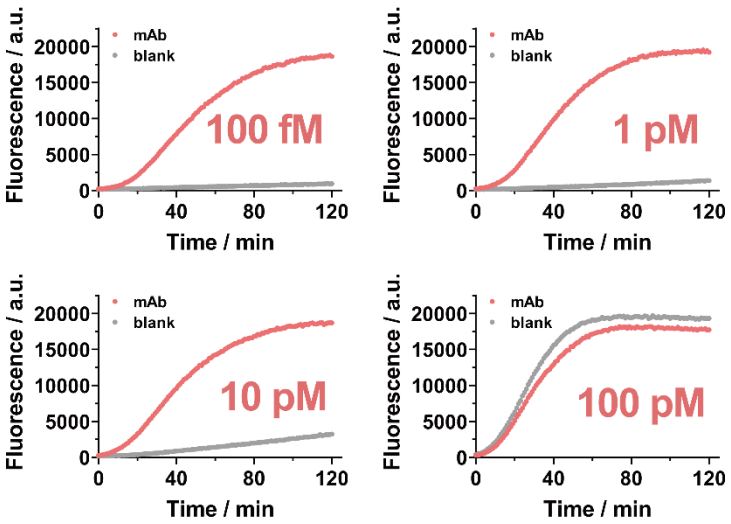

Figure S3 | Optimization of UCAD probe concentration. Optimization of UCAD probe concentration in detecting anti-RBD mAb. Despite 1 pM TS and NTS probe concentration demonstrates the best signal to background ratio, 10 pM was chosen as the optimal TS and NTS probe concentration to maximize the dynamic range for the detection of anti-RBD mAb. [mAb] = 100 fM, [T4 polymerase] = 2 U, [dNTPs]= 40 μM, [Cas12a] = 40 nM, [crRNA] = 40 nM, [Reporter] = 40 nM.

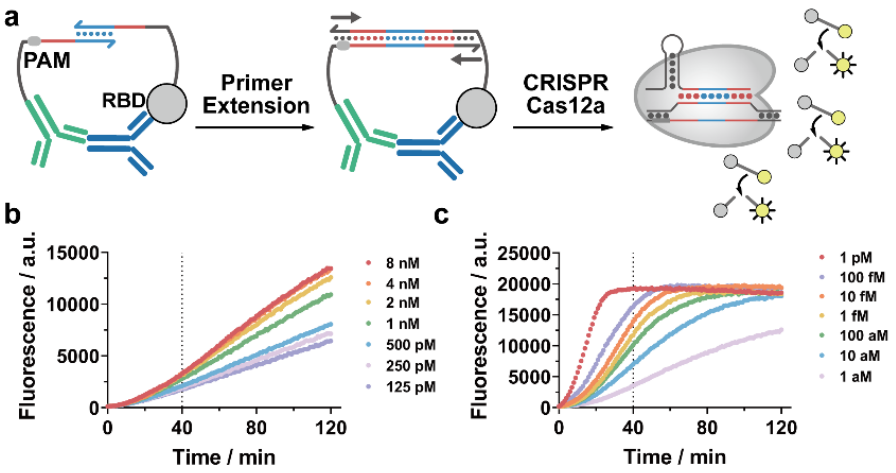

Figure S4 | Sensitivity of UCAD in buffer. (**a**) Schematic illustration of UCAD workflow in detecting anti-RBD human mAb without nucleic acid amplification of the pre-designed dsDNA barcode. (**b**) Kinetic curves for mAb detection using UCAD without RPA. The concentrations of mAb were ranged from 125 pM to 8 nM. (**c**) Kinetic curves for mAb detection using UCAD with RPA. The concentration of mAb were ranged from 1 aM to 1pM. [TS probe] = 10 pM, [NTS probe] = 10 pM, [T4 polymerase] = 2 U, [dNTPs]= 40 μM, [Cas12a] = 40 nM, [crRNA] = 40 nM, [FQ-labeled reporter] = 40 nM.

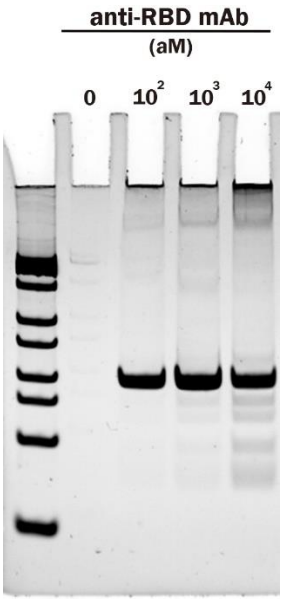

Figure S5 | Native PAGE analysis of UCAD. Native PAGE analysis of the regeneration and RPA amplification of dsDNA barcode for UCAD. The optimal workflow for UCAD was used to regenerate and amplify dsDNA barcode in response to 100 aM to 10 fM anti-RBD mAb. RPA amplicon was analyzed using 12% PAGE gel. 1 μL of UCAD product was mixed with 5 μL loading buffer before loading on gel. After electrophoresing in 1× TAE buffer at 120 V for 1 h, the gel was stained using Gel Red and visualized using GenoSens 2000 (CLINX) gel imaging system. From left to right: Lane 1: 25 – 500 bp DNA ladder, Lane 2: reaction buffer containing no anti-RBD mAb (Blank), Lane 3: reaction buffer containing 100 aM anti-RBD mAb, Lane 4: reaction buffer containing 1 fM anti-RBD mAb, Lane 5: reaction buffer containing 10 fM anti-RBD mAb. Reaction buffer: [TS probe] = 10 pM, [NTS probe] = 10 pM, [dNTPs]= 40 μM, [T4 polymerase] = 2 U.

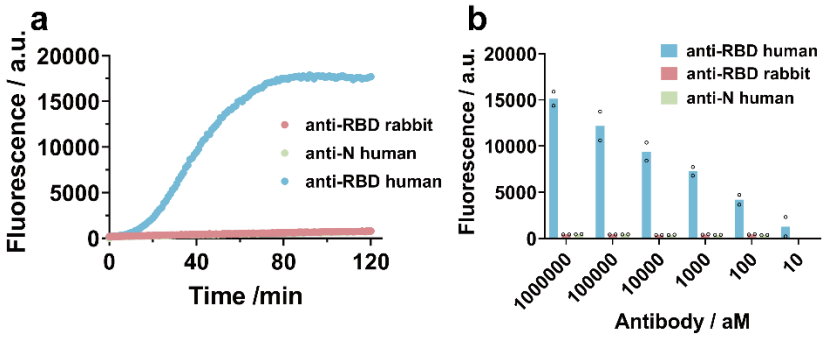

Figure S6 | Specificity of UCAD. Evaluating the specificity of UCAD for anti-human RBD (anti-RBD human) against closely related anti-rabbit RBD (anti-RBD rabbit) and anti-human SARS-CoV-2 N nucleocapsid protein (anti-N human). the anti-SARS-CoV-2 Spike protein RBD human mAb. (**a**) UCAD kinetic curves for 10 fM anti-human RBD against equal concentrations of nonspecific antibodies. (**b**) Detection of anti-human RBD and nonspecific antibodies in the concentration range from 1 pM to 10 aM using UCAD. Only anti-RBD human mAb generated fluorescence signal linearly correlated with its concentration. [TS probe] = 10 pM, [NTS probe] = 10 pM, [T4 polymerase] = 2 U, [dNTPs]= 40 μM, [Cas12a] = 40 nM, [crRNA] = 40 nM, [Reporter] = 40 nM.

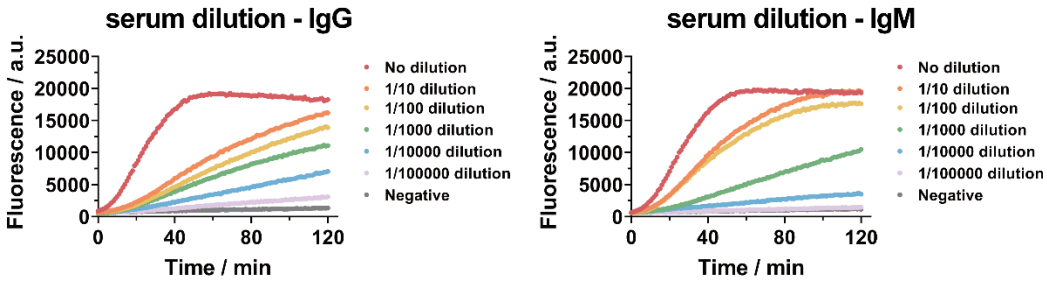

Figure S7 | Sensitivity of UCAD in human serum samples. Detection of anti-RBD IgG (**a**) and IgM (**b**) in certified anti-SARS-CoV-2 positive human serum sample and diluted sera using certified COVID-19 negative human serum sample. [TS probe] = 10 pM, [NTS probe] = 10 pM, [T4 polymerase] = 2 U, [dNTPs]= 40 μM, [Cas12a] = 40 nM, [crRNA] = 40 nM, [FQ-labeled reporter] = 40 nM.

S2. Engineering of lateral flow readout for UCAD.

Fabricate lateral flow strips: The lateral flow strip was assembled by four components: the sample pad, the conjugate pad, the nitrocellulose membrane (Whatman®, purchased from Sigma Aldrich) and the absorbent pad. The sample pad was saturated with a buffer containing 0.25 % Triton X-100, 0.05 M Tris-HCl, and 0.15 M NaCl. Optimized volume of AuNPs-anti-FAM conjugates were loaded on the conjugate pad. Digoxin rabbit polyclonal antibody was dispensed on the nitrocellulose membrane at the control (C) line, and the goat anti-rabbit IgG was dispensed at the test (T) line using the XYZ platform dispenser HM3030 (Shanghai Kinbio Tech Co., Ltd.). All the membranes and pads were dried at 37 °C for 2 h before assembled and cut.

Lateral flow readout of UCAD. To fabricate UCAD into a point-of-care (POC) setting for the serology test for COVID-19, we replaced the fluorophore-quencher labeled fluorogenic ssDNA reporters for Cas12a to a ssDNA reporter labeled with FAM at one end and digoxin (Dig) at the other. A lateral flow test strip was then constructed with anti-Dig immobilized at the control line (C-line) and goat anti-rabbit IgG at the test line (T-line). In the absence of the target antibodies, the FAM-Dig labeled ssDNA reporter remains intact, which helps capture all rabbit anti-FAM labeled gold nanoparticles (AuNPs) at the C-line. In the presence of the anti-RBD IgG or IgM, the ssDNA reporters were cleaved by the target-induced collateral activity of Cas12a. As a result, AuNPs were captured at the T-line. By visually examining the results in Figure S32c and S32d, we were able to clearly identify 15 anti-SARS-CoV-2 positive clinical sera from 7 pre-pandemic negative sera.

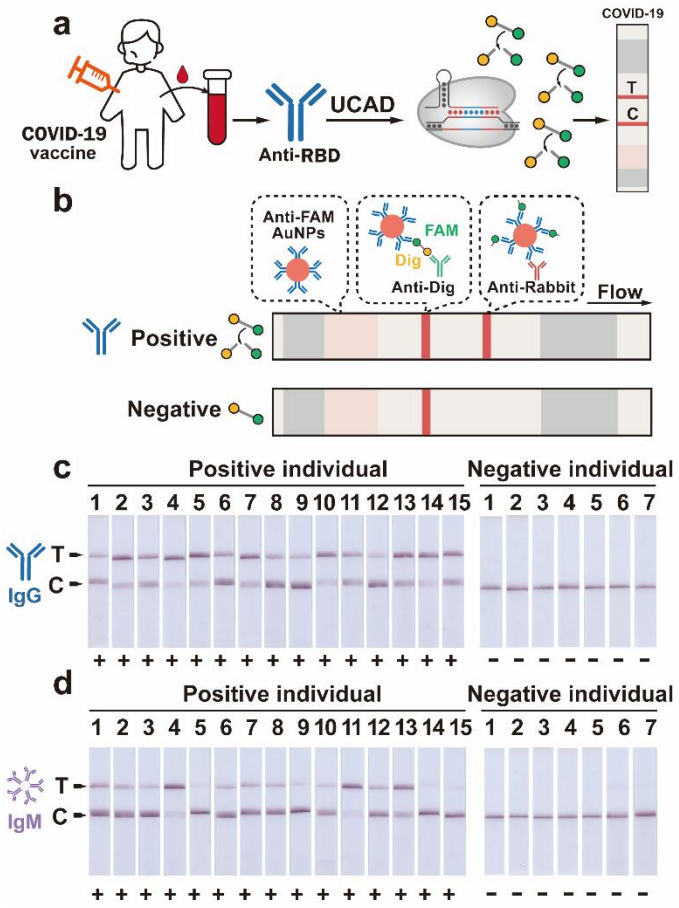

Figure S8 | UCAD with lateral flow readout. (**a**) UCAD workflow for detecting anti-RBD IgG and IgM in serum samples collected from vaccinated healthy participates with lateral flow readouts. (**b**) In the presence of anti-RBD IgG or IgM, the FAM-Dig reporters were cleaved by Cas12a-crRNA. The cleaved reporter bounded anti-FAM AuNPs could flow through the control line (C-line) immobilized with anti-Dig antibodies and accumulated at test line (T-line) through binding with the immobilized secondary antibody. For negative samples, the reporters are intact as the trans-cleavage of Cas-12a-crRNA was not activated, thereby the intact reporter bounded anti-FAM AuNPs were captured by anti-Dig antibody on C-line rather than the T-line. (**c, d**) Visual readout of anti-RBD IgG (**c**) and IgM (**d**) in the clinical positive and negative sera by UCAD integrated with lateral flow strips.

S3. Demographic and vaccination information of KTRs

Table S2. Vaccination information of 85 KTRs.

sample #	age	gender	sampling day	1st Dose	2nd Dose	CLIA-IgG (S/CO*)	CLIA-IgM (S/CO)
1	35	M	40	BBIBP-CorV	BBIBP-CorV	n.d.**	n.d.
2	45	M	20	CoronaVac	CoronaVac	n.d.	n.d.
3	52	M	26	CoronaVac	BBIBP-CorV	n.d.	n.d.
4	28	M	40	BBIBP-CorV	BBIBP-CorV	n.d.	n.d.
5	48	F	24	CoronaVac	CoronaVac	n.d.	n.d.
6	51	M	41	BBIBP-CorV	BBIBP-CorV	n.d.	n.d.
7	49	M	40	CoronaVac	CoronaVac	1.35***	n.d.
8	46	F	40	BBIBP-CorV	BBIBP-CorV	n.d.	n.d.
9	43	M	29	BBIBP-CorV	BBIBP-CorV	n.d.	n.d.
10	57	M	29	CoronaVac	CoronaVac	n.d.	n.d.
11	35	F	43	BBIBP-CorV	BBIBP-CorV	n.d.	n.d.
12	53	M	41	BBIBP-CorV	BBIBP-CorV	n.d.	n.d.
13	26	F	27	CoronaVac	CoronaVac	n.d.	n.d.
14	30	M	57	CoronaVac	CoronaVac	1.98	1.09
15	52	F	32	CoronaVac	CoronaVac	n.d.	n.d.
16	42	M	15	CoronaVac	CoronaVac	n.d.	n.d.
17	22	F	36	CoronaVac	BBIBP-CorV	n.d.	1.13
18	52	F	44	CoronaVac	CoronaVac	n.d.	n.d.
19	43	M	21	BBIBP-CorV	BBIBP-CorV	n.d.	n.d.
20	52	M	43	CoronaVac	CoronaVac	n.d.	n.d.
21	41	M	27	CoronaVac	CoronaVac	0.5	0.53
22	42	M	21	CoronaVac	CoronaVac	n.d.	n.d.
23	46	F	24	CoronaVac	CoronaVac	0.1	n.d.
24	37	F	23	BBIBP-CorV	BBIBP-CorV	n.d.	n.d.
25	34	F	26	BBIBP-CorV	BBIBP-CorV	n.d.	n.d.
26	38	M	33	BBIBP-CorV	BBIBP-CorV	n.d.	n.d.
27	43	M	29	CoronaVac	CoronaVac	n.d.	n.d.
28	24	M	39	BBIBP-CorV	BBIBP-CorV	0.11	n.d.
29	44	M	16	CoronaVac	BBIBP-CorV	n.d.	n.d.
30	24	M	26	CoronaVac	CoronaVac	0.54	0.32
31	42	M	18	CoronaVac	CoronaVac	0.88	0.11
32	41	M	31	BBIBP-CorV	BBIBP-CorV	n.d.	n.d.
33	30	M	35	BBIBP-CorV	BBIBP-CorV	1.95	0.47
34	53	M	24	CoronaVac	CoronaVac	n.d.	n.d.
35	44	F	22	CoronaVac	CoronaVac	n.d.	n.d.
36	56	M	16	CoronaVac	CoronaVac	0.35	n.d.

37	39	M	27	BBIBP-CorV	BBIBP-CorV	n.d.	n.d.
38	55	M	15	CoronaVac	CoronaVac	n.d.	n.d.
39	48	M	31	CoronaVac	CoronaVac	n.d.	n.d.
40	43	M	43	CoronaVac	CoronaVac	n.d.	n.d.
41	31	M	36	BBIBP-CorV	BBIBP-CorV	0.12	n.d.
42	59	M	21	BBIBP-CorV	BBIBP-CorV	n.d.	n.d.
43	42	F	23	BBIBP-CorV	CoronaVac	0.28	n.d.
44	50	M	15	BBIBP-CorV	CoronaVac	n.d.	0.29
45	27	M	44	BBIBP-CorV	CoronaVac	n.d.	2.14
46	44	M	18	CoronaVac	BBIBP-CorV	n.d.	n.d.
47	47	M	14	BBIBP-CorV	CoronaVac	n.d.	0.2
48	58	M	34	BBIBP-CorV	BBIBP-CorV	n.d.	n.d.
49	21	M	17	BBIBP-CorV	BBIBP-CorV	n.d.	n.d.
50	66	M	20	CoronaVac	CoronaVac	n.d.	n.d.
51	44	M	32	CoronaVac	CoronaVac	n.d.	n.d.
52	45	F	15	BBIBP-CorV	CoronaVac	n.d.	n.d.
53	33	F	39	BBIBP-CorV	BBIBP-CorV	n.d.	n.d.
54	54	M	17	BBIBP-CorV	BBIBP-CorV	n.d.	n.d.
55	51	M	16	BBIBP-CorV	BBIBP-CorV	n.d.	n.d.
56	55	M	39	CoronaVac	CoronaVac	n.d.	n.d.
57	29	M	12	CoronaVac	BBIBP-CorV	n.d.	n.d.
58	35	M	14	CoronaVac	CoronaVac	n.d.	n.d.
59	33	M	13	BBIBP-CorV	BBIBP-CorV	0.1	n.d.
60	35	F	22	CoronaVac	BBIBP-CorV	n.d.	n.d.
61	48	M	39	CoronaVac	CoronaVac	n.d.	n.d.
62	27	M	20	CoronaVac	BBIBP-CorV	n.d.	n.d.
63	44	M	19	CoronaVac	BBIBP-CorV	n.d.	n.d.
64	42	M	36	BBIBP-CorV	BBIBP-CorV	n.d.	n.d.
65	50	M	50	CoronaVac	CoronaVac	n.d.	n.d.
66	41	F	18	CoronaVac	CoronaVac	n.d.	n.d.
67	47	M	59	CoronaVac	BBIBP-CorV	n.d.	n.d.
68	51	M	33	CoronaVac	CoronaVac	n.d.	n.d.
69	48	M	16	BBIBP-CorV	BBIBP-CorV	n.d.	n.d.
70	44	M	20	BBIBP-CorV	BBIBP-CorV	n.d.	n.d.
71	44	M	19	CoronaVac	BBIBP-CorV	n.d.	n.d.
72	49	M	17	CoronaVac	CoronaVac	n.d.	n.d.
73	32	M	19	CoronaVac	CoronaVac	n.d.	n.d.
74	35	F	15	CoronaVac	BBIBP-CorV	n.d.	n.d.
75	33	F	13	CoronaVac	CoronaVac	n.d.	n.d.
76	29	F	22	BBIBP-CorV	CoronaVac	0.33	n.d.

77	49	M	17	CoronaVac	CoronaVac	n.d.	n.d.
78	44	M	13	CoronaVac	CoronaVac	n.d.	n.d.
79	38	F	62	BBIBP-CorV	BBIBP-CorV	n.d.	n.d.
80	34	M	41	CoronaVac	CoronaVac	n.d.	0.62
81	30	F	35	BBIBP-CorV	BBIBP-CorV	n.d.	n.d.
82	56	F	31	BBIBP-CorV	BBIBP-CorV	n.d.	n.d.
83	46	M	57	CoronaVac	CoronaVac	n.d.	0.15
84	53	F	27	CoronaVac	BBIBP-CorV	n.d.	n.d.
85	35	F	16	CoronaVac	CoronaVac	n.d.	n.d.

*S/CO stands Signal/Cut-off.

**n.d. stands for nondetectable and clinically defined to be negative (S/CO < 0.1).

***Anti-RBD IgG or IgM positive was clinically defined to be S/CO ≥ 1.

Table S3. Demographic characteristics of 85 KTRs.

	IgG^+/IgM^+ (n=73)	IgG^-/IgM^- (n=12)
Donor type		
Living	29(39.7%)	8(66.7%)
Deceased	44(60.3%)	4(33.3%)
Recipient gender		
Male	54(74.0%)	7(58.3%)
Female	19(26.0%)	5(41.7%)
Age (year)	41.9±11.1	40.3±7.2
Transplantation to vaccination (month)	114±73	119±88
Sample from vaccination (day)	29±14	28±17
Induction therapy		
No	6(8.2%)	2(16.7%)
ATG/ATGF	22(30.1%)	5(41.7%)
Basiliximab	45(61.6%)	5(41.7%)
Steroid pulse therapy in 12 months		
Yes	1(1.4%)	0
No	72(98.6%)	0
ATG (anti-thymocyte globulin therapy) in 12 months		
Yes	1(1.4%)	0
No	72(98.6%)	0
eGFR (estimated glomerular filtration rate) before vaccination (ml/min)	64±19	70±11
Albumin before vaccination (g/L)	45.5±3.4	46.8±2.8
Globulin before vaccination (g/L)	24.2±4.1	23.9±2.5
Hemoglobulin before vaccination (g/L)	143±19	140±17
WBC (white blood cell) before vaccination (10^9/L)	7.5±2.4	7.2±1.6
Neutrophil before vaccination (10^9/L)	4.9±1.9	4.6±1.1
Lymphocyte before vaccination (10^9/L)	1.9±0.7	1.9±0.5
Tacrolimus trough level before vaccination (ng/ml)	5.9±1.6	5.2±2.0

S4. UCAD analysis of KTRs

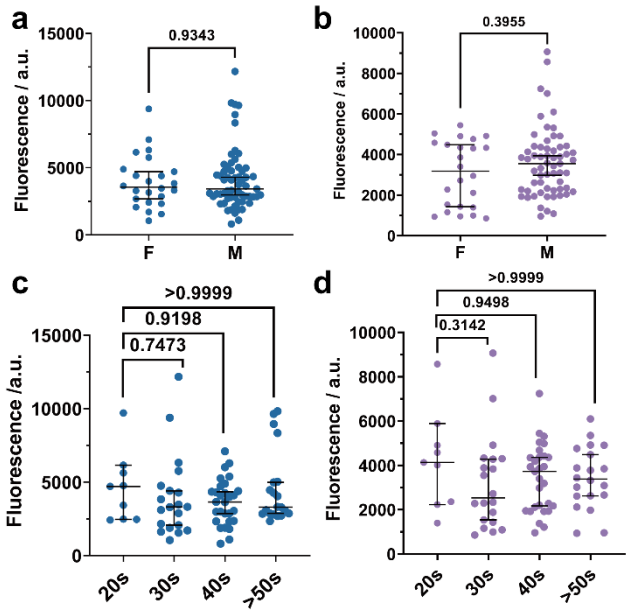

Figure S9 | Correlation of anti-RBD level with gender and age. (**a, b**) Correlation of UCAD-determined anti-RBD IgG (**a**) and IgM (**b**) levels of 85 KTRs with gender. Female: 24, Male: 61. No significant differences in the levels of anti-RBD IgG and IgM were found between genders. (**c, d**) Correlation of the UCAD-determined anti-RBD IgG (**c**) and IgM (**d**) levels of 85 KTRs with age. No significant differences were found between varying age groups. Comparison of anti-RBD IgG and IgM levels between two gender groups were performed using unpaired t-test. Kruskal-Wallis test was used to evaluate the differences of the IgG and IgM levels between four age groups.

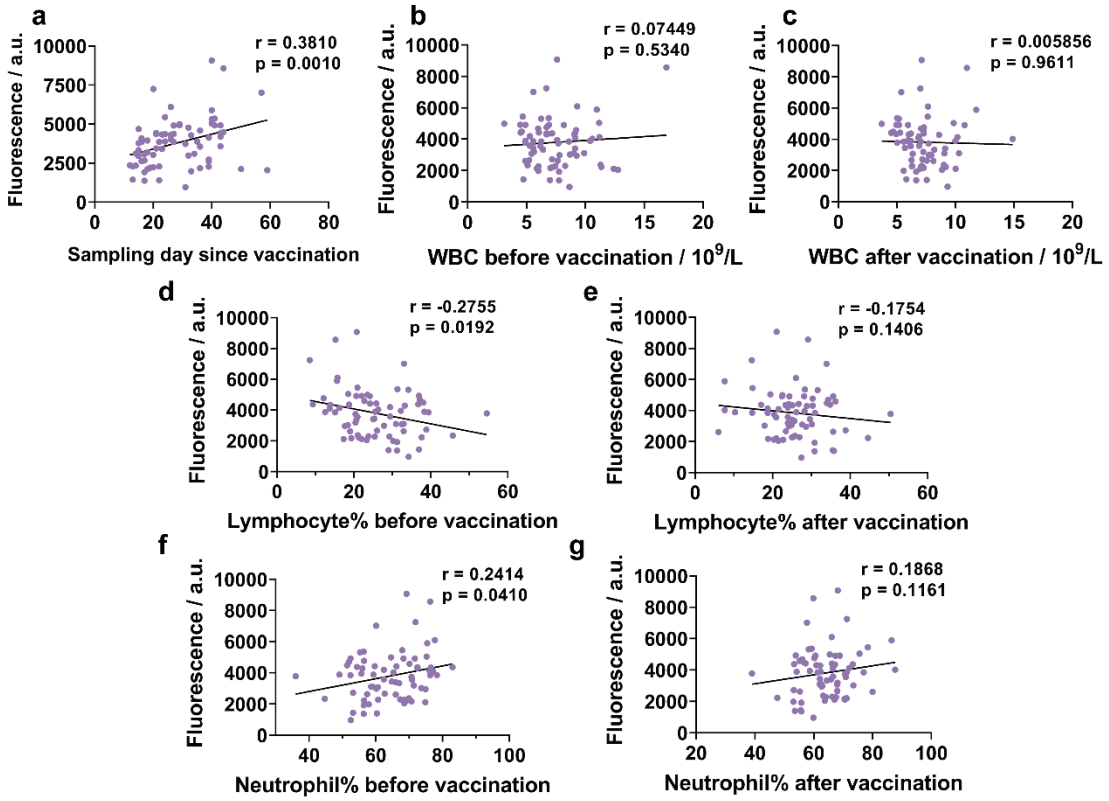

Figure S10 | Correlation of UCAD-determined IgM with vaccination program. (**a**) Spearman correlation analysis to evaluate the relationship between the UCAD-determined IgM levels of 73 anti-RBD positive KTRs and sampling days since vaccination. A significant positive correlation between anti-RBD IgM levels and the sampling day with a p value of 0.001 (r = 0.3810, n = 73). (**b, c**) Pearson correlation analysis of the UCAD-determined anti-RBD IgM level and counts of WBC before (**b**) and after (**c**) COVID-19 vaccination. No significant differences were found between IgM levels and WBC counts either before (p = 0.5340) or after (p = 0.9611) vaccination. (**d, e**) Pearson correlation analysis of the UCAD-determined IgM levels and the percentage composition of lymphocytes in WBC before (**d**) and after (**e**) vaccination. A significant negative correlation between anti-RBD IgM level and percentage composition of lymphocyte before vaccination (**d**) was found with p value of 0.0192 (r = -0.2755, n = 73). No significant correlation between anti-RBD IgM level and percentage

composition of lymphocyte after vaccination (**c**) was found ($p = 0.1406$, $n = 73$). (**f, g**) Pearson correlation analysis of the UCAD-determined IgM levels and the percentage composition of neutrophils in WBC before (**f**) and after (**g**) vaccination. A positive correlation between anti-RBD IgM level and percentage composition of neutrophil before vaccination was found with a baseline p value of 0.041 ($r = 0.2414$, $n = 73$). No significant correlation between anti-RBD IgM level and percentage composition of neutrophil after vaccination ($p = 0.1161$, $n = 73$).

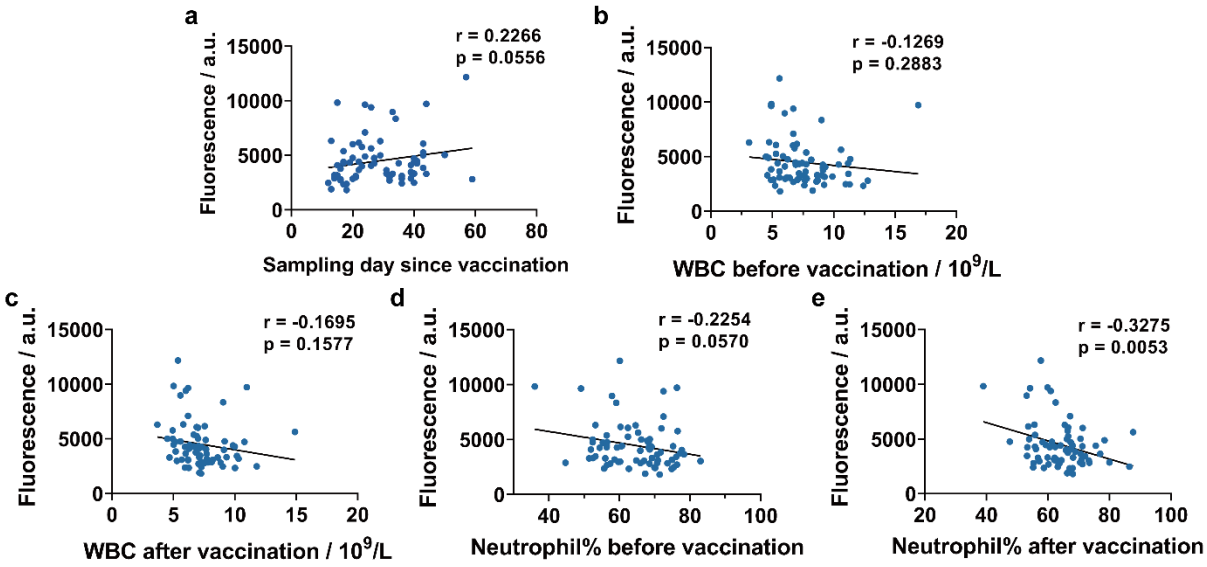

Figure S11 | Correlation of UCAD-determined IgG with vaccination program. (**a**) Spearman correlation analysis to evaluate the relationship between the UCAD-determined IgG levels of 73 anti-RBD positive KTRs and sampling days since vaccination. A weak positive correlation between anti-RBD IgG levels and the sampling day with a baseline p value of 0.0556 (r = 0.2266, n = 73). (**b, c**) Pearson correlation analysis of the UCAD-determined anti-RBD IgG level and counts of white blood cell (WBC) before (**b**) and after (**c**) COVID-19 vaccination. No significant differences were found between IgG levels and WBC counts either before (p = 0.2883) or after (p = 0.1577) vaccination. (**d, e**) Pearson correlation analysis of the UCAD-determined IgG levels and the percentage composition of neutrophils in WBC before (**d**) and after (**e**) vaccination. A weak negative correlation between anti-RBD IgG level and percentage composition of neutrophil before vaccination (**d**) was found with a baseline p value of 0.057 (r = -0.2254, n = 73). A significant negative correlation between anti-RBD IgG level and percentage composition of neutrophil after vaccination (**e**) was found with a p value of 0.0053 (r = -0.3275, n = 73).

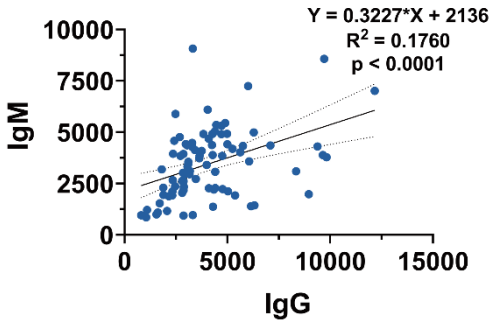

Figure S12 | Linear correlation between UCAD-determined IgG and IgM in KTRs.

Levels of UCAD-determined anti-RBD IgG and IgM were found to be linearly correlated in 85 KTRs ($p < 0.0001$).

S5. Cellular analysis of KTRs

Blood samples from seven anti-RBD positive vaccinated KTRs (P1, P2, P3, P4, P5, P6, P7), five anti-RBD negative KTRs (N1, N2, N3, N4, N5), as well as five anti-RBD positive sera from vaccinated healthy participates (H1, H2, H3, H4, H5) were analyzed using flow cytometry to determine the distribution of B and Th cell subsets.

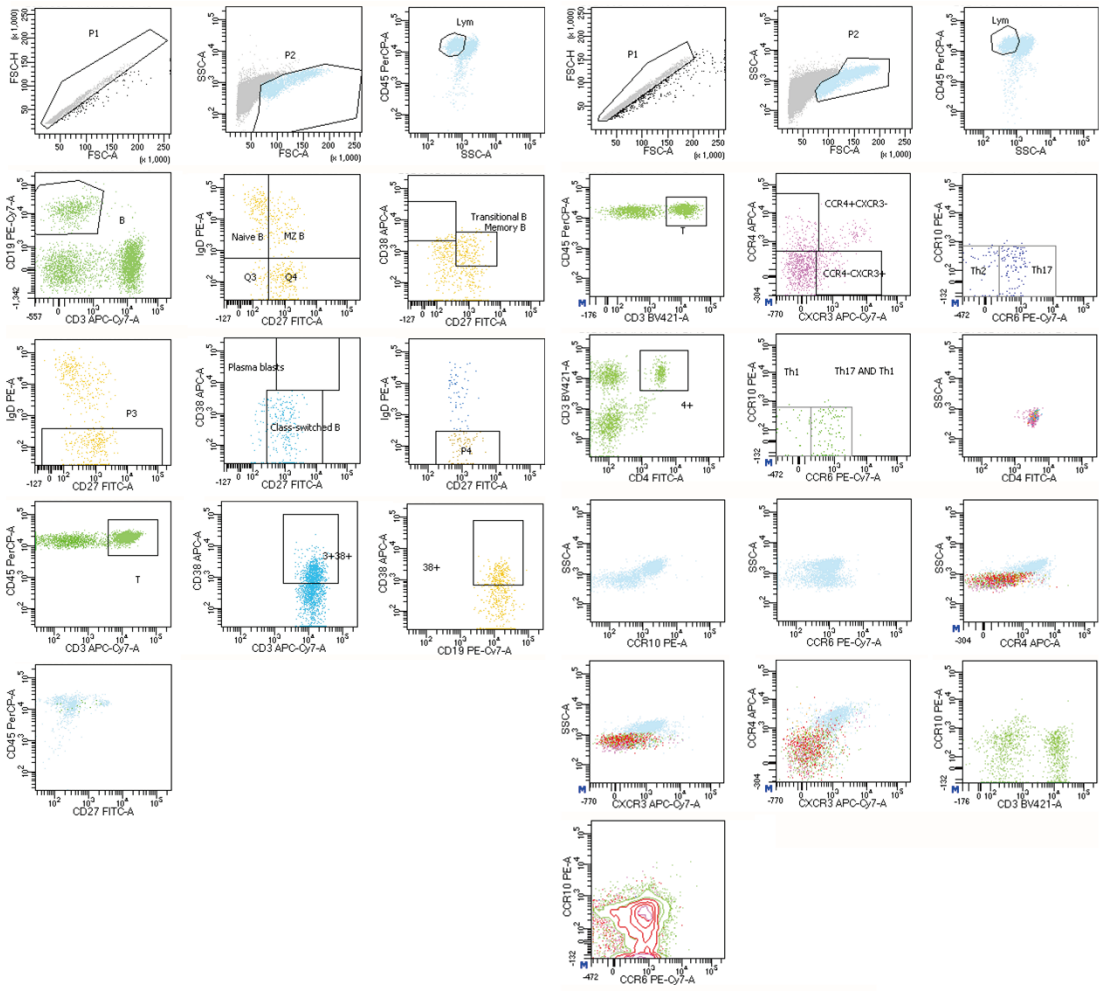

Figure S13 | Flow cytometry analysis of B cell and Th cell subsets in P1.

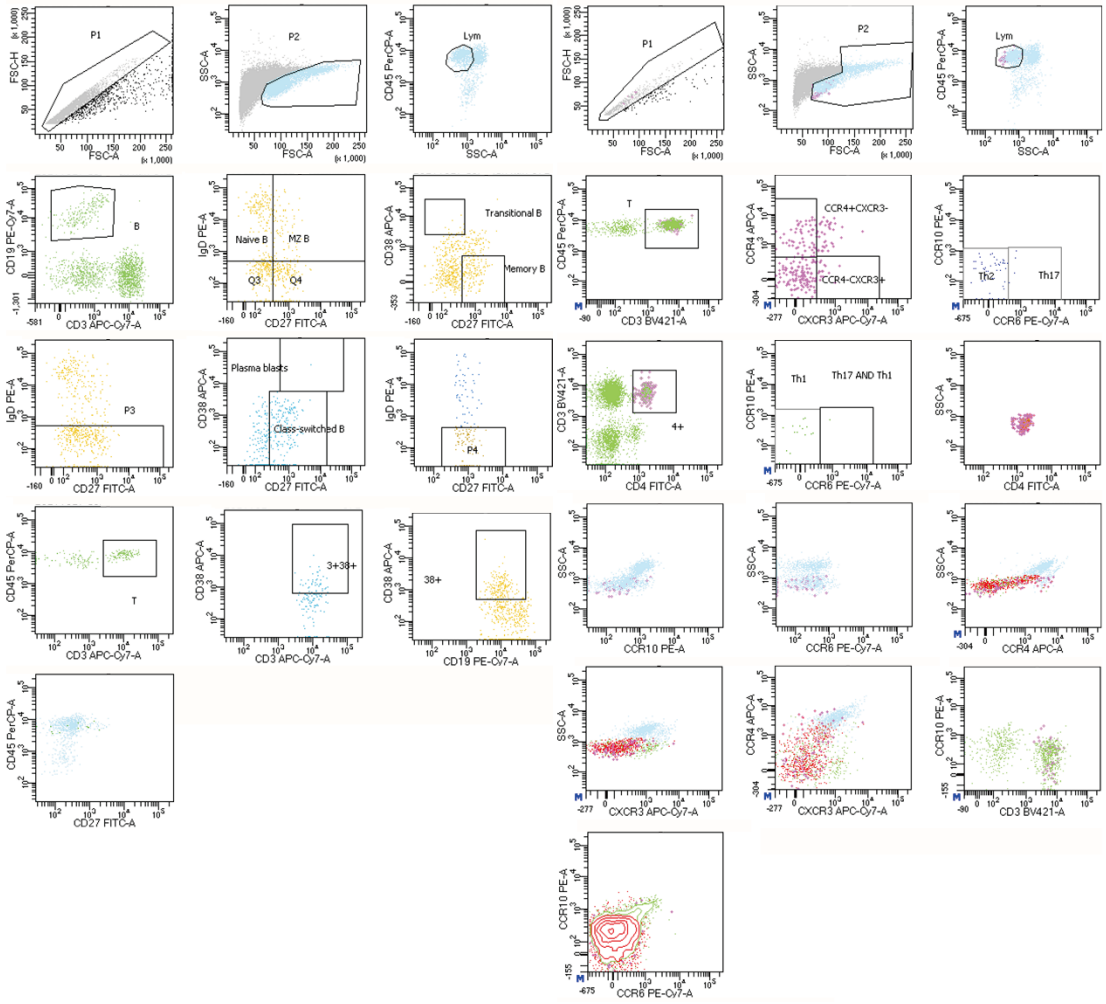

Figure S14 | Flow cytometry analysis of B cell and Th cell subsets in P2.

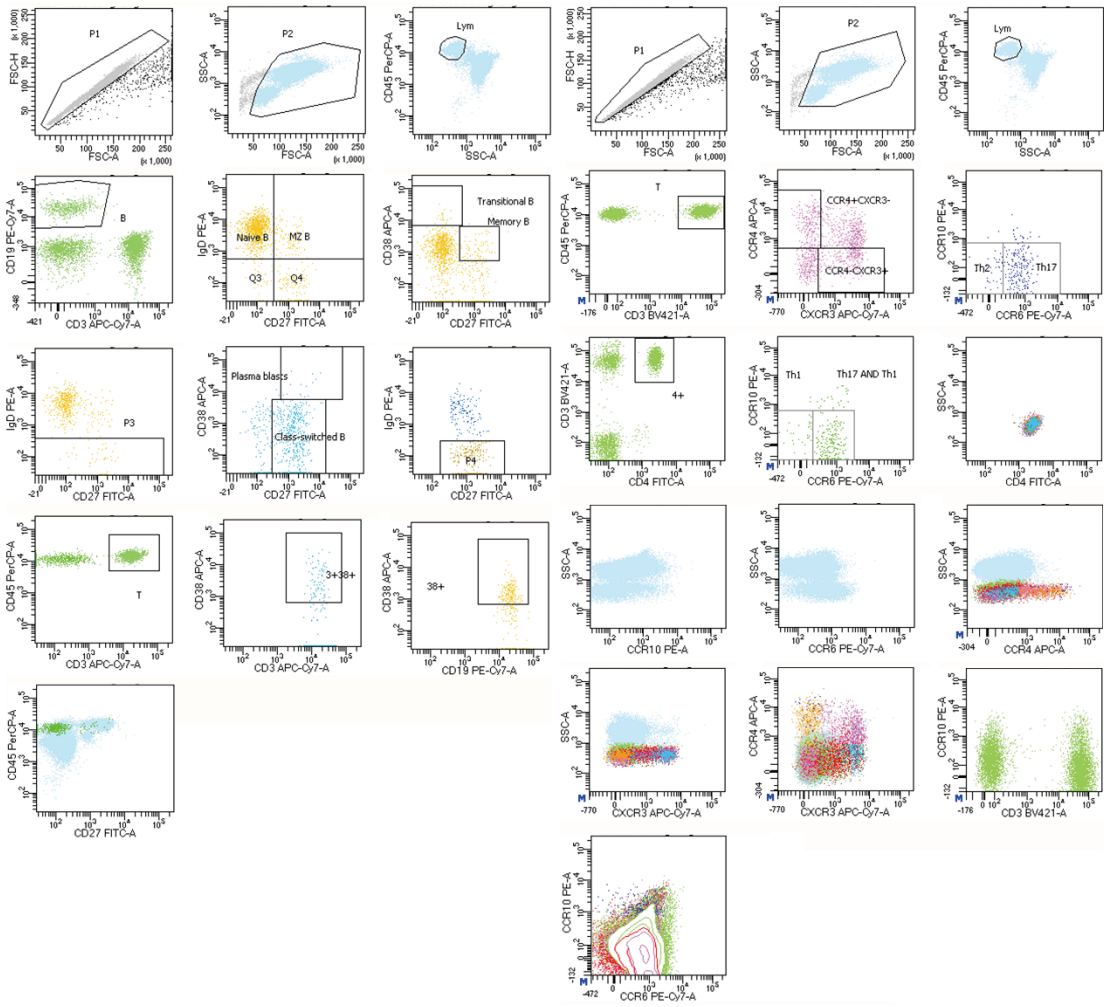

Figure S15 | Flow cytometry analysis of B cell and Th cell subsets in P3.

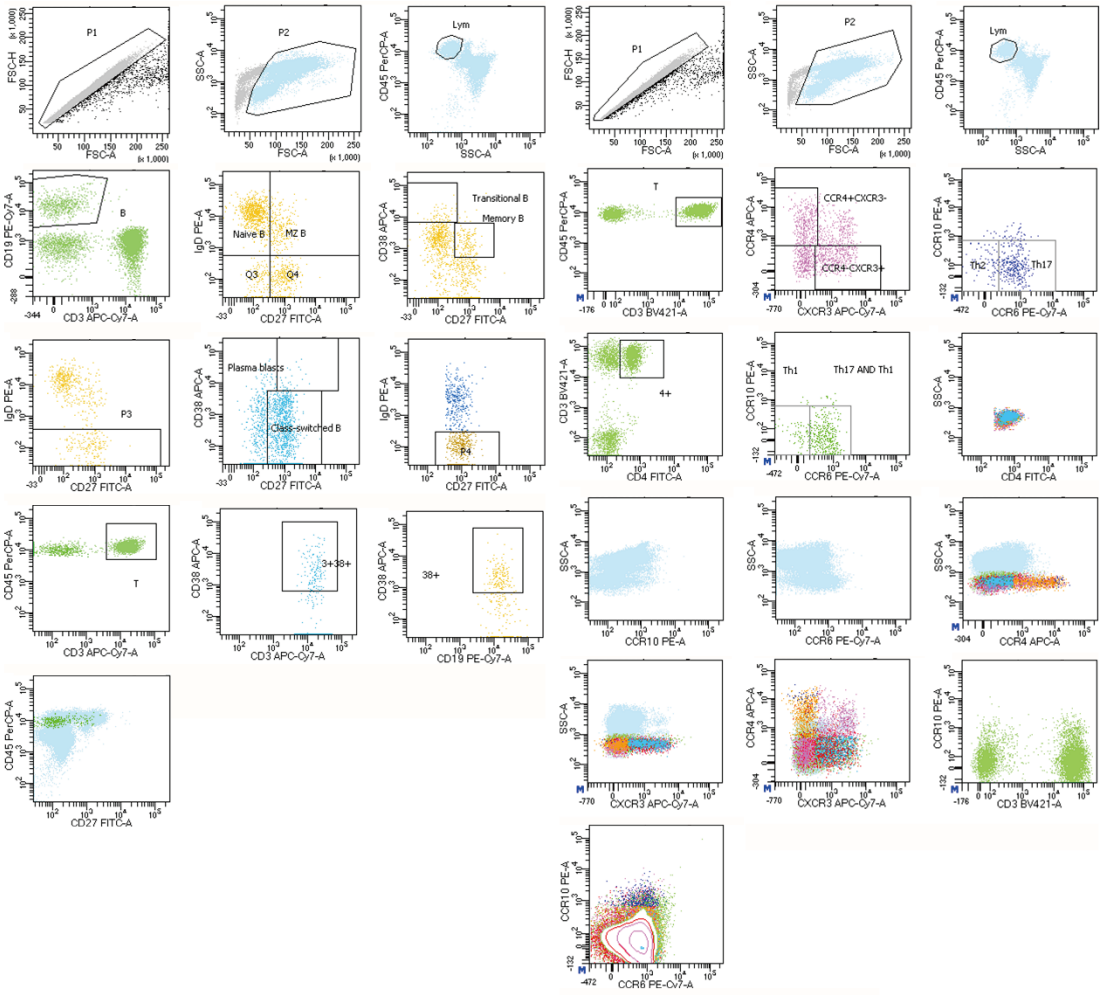

Figure S16 | Flow cytometry analysis of B cell and Th cell subsets in P4.

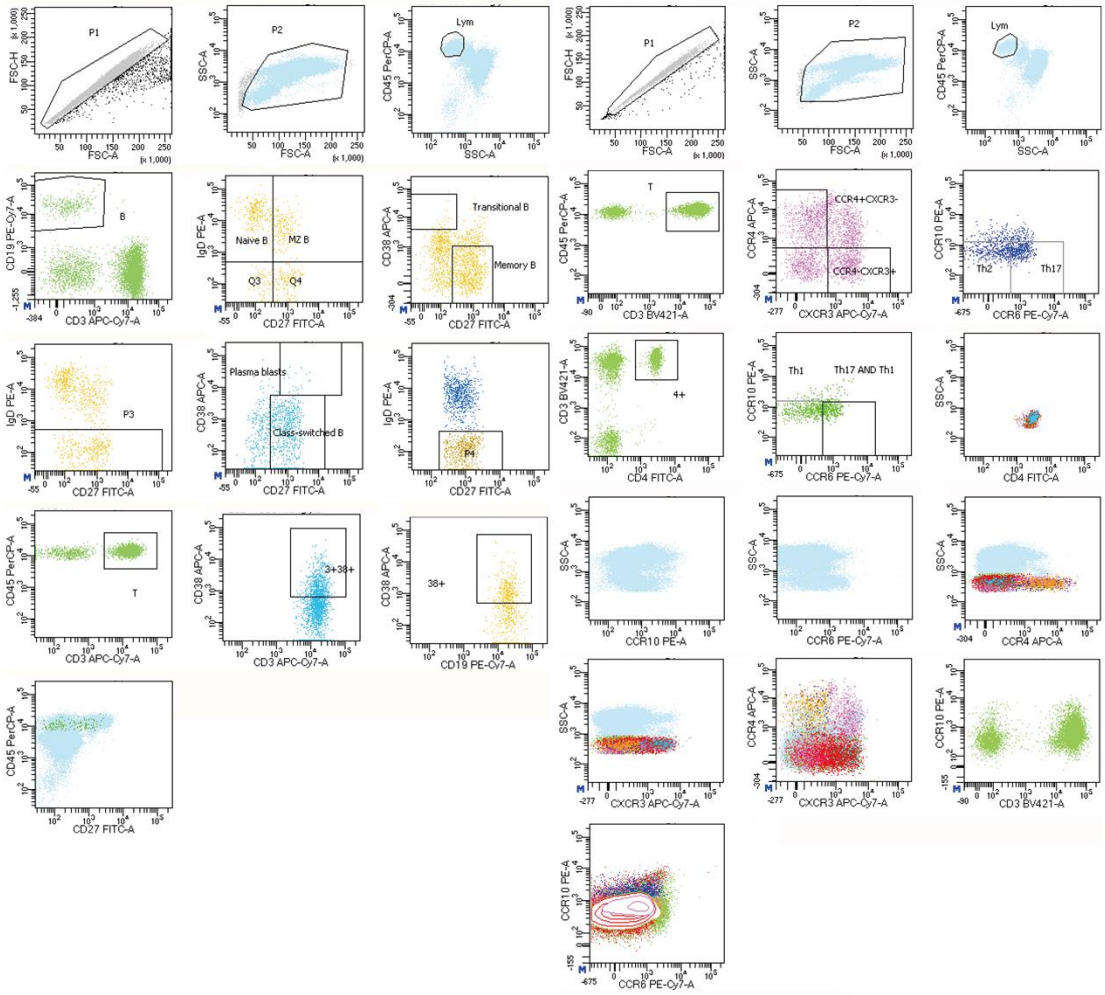

Figure S17 | Flow cytometry analysis of B cell and Th cell subsets in P5.

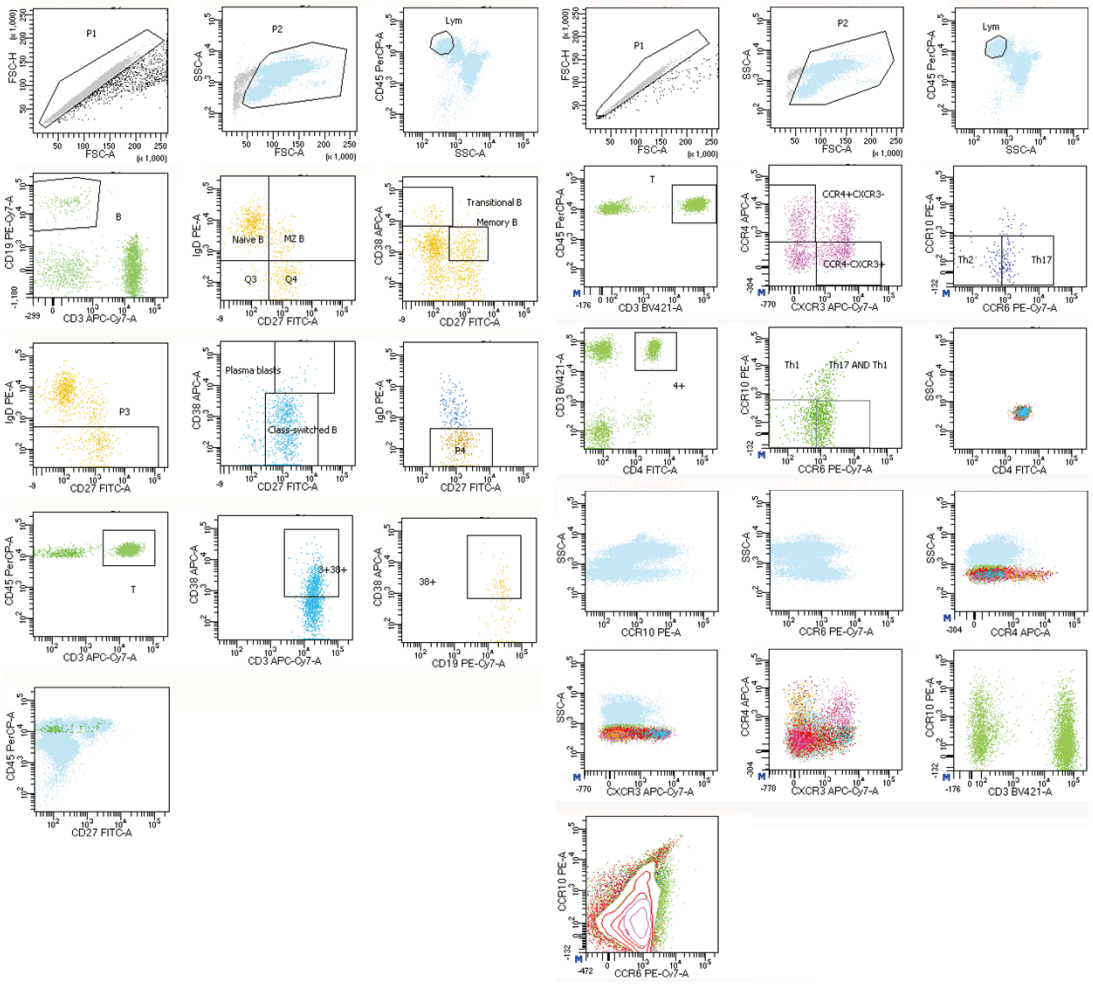

Figure S18 | Flow cytometry analysis of B cell and Th cell subsets in P6.

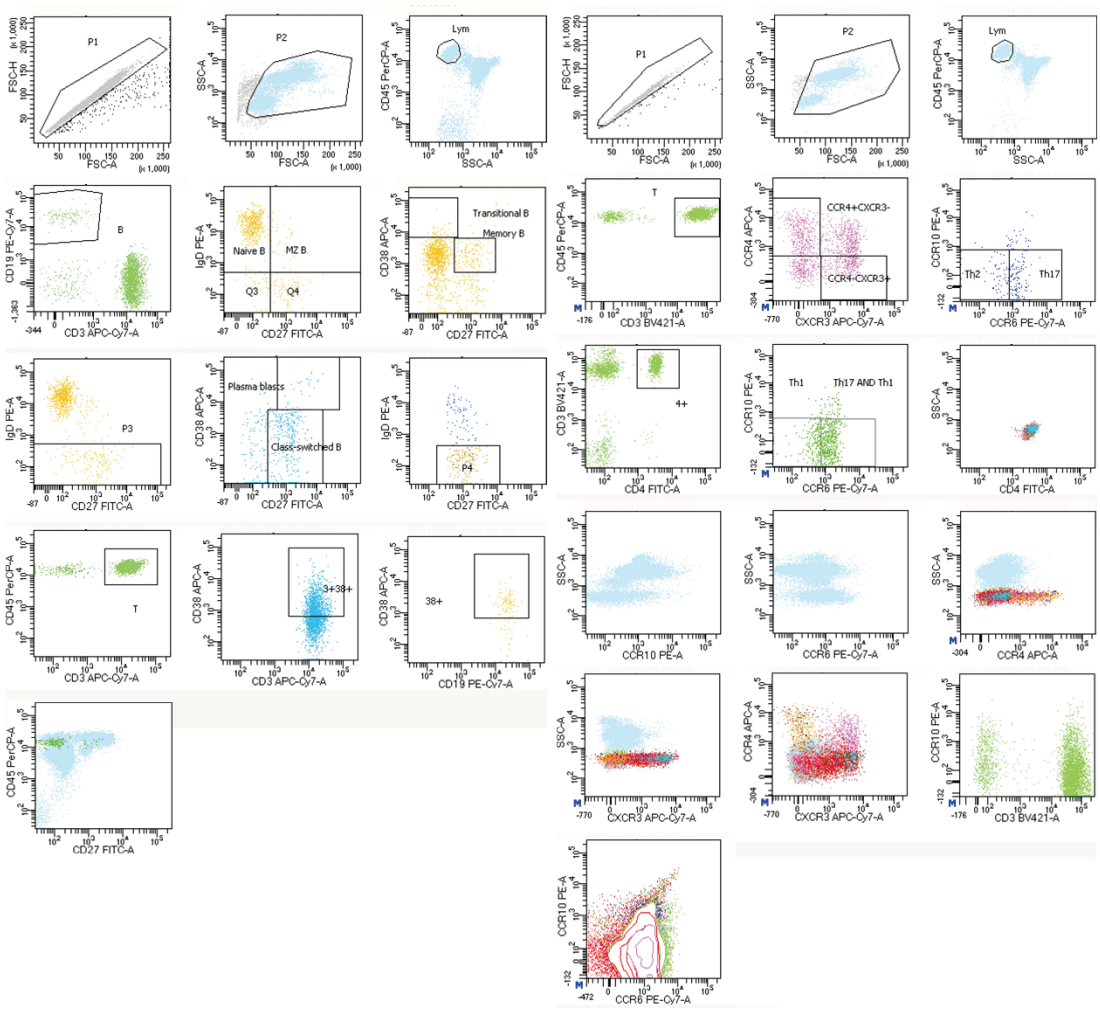

Figure S19 | Flow cytometry analysis of B cell and Th cell subsets in P7.

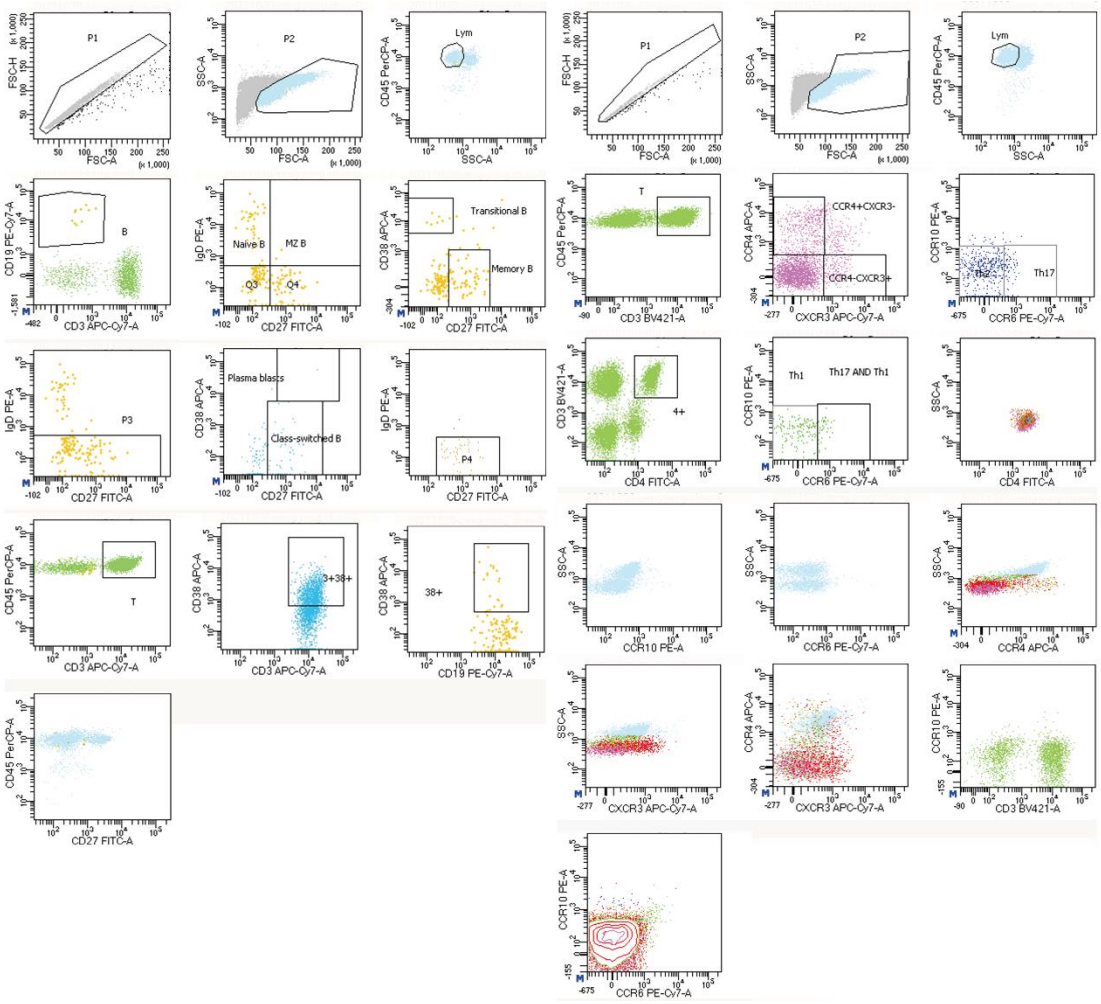

Figure S20 | Flow cytometry analysis of B cell and Th cell subsets in N1.

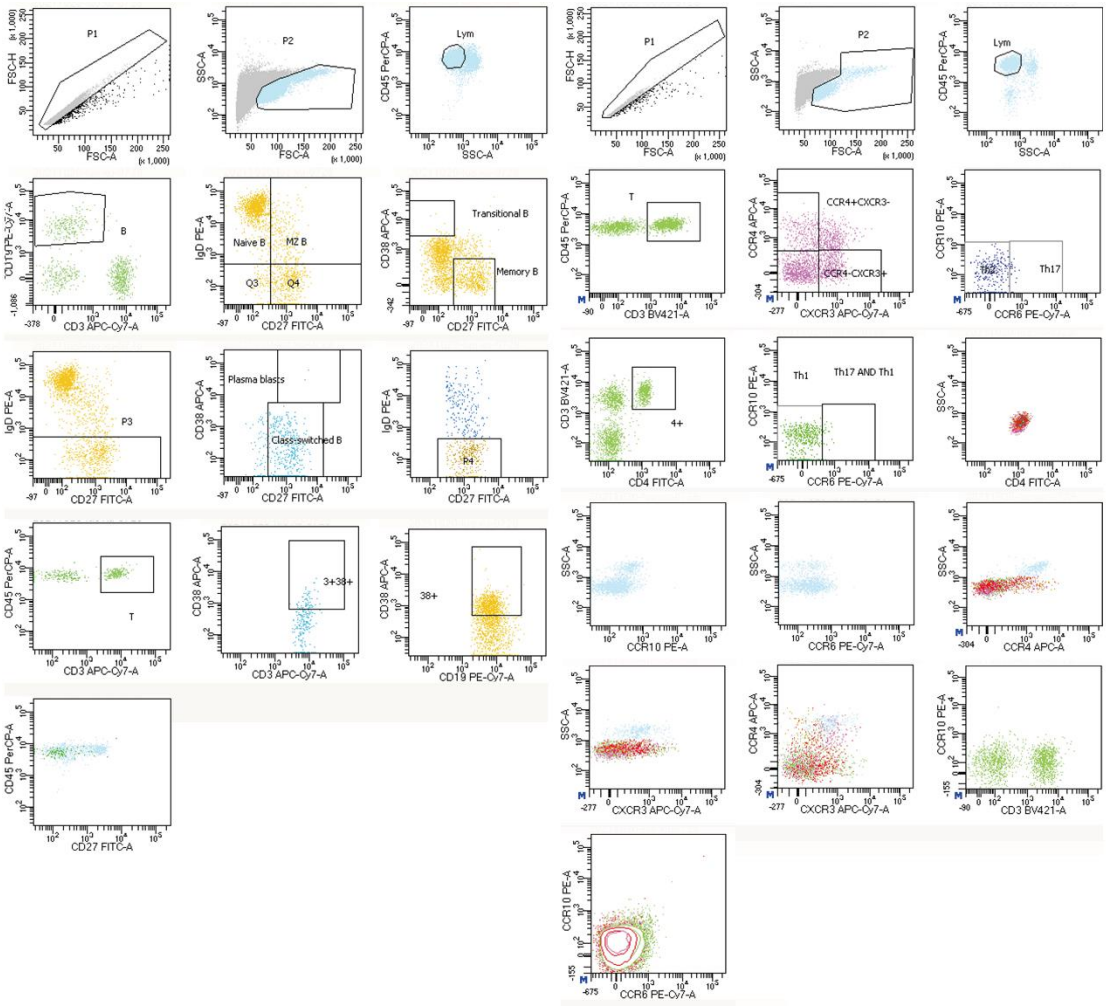

Figure S21 | Flow cytometry analysis of B cell and Th cell subsets in N2.

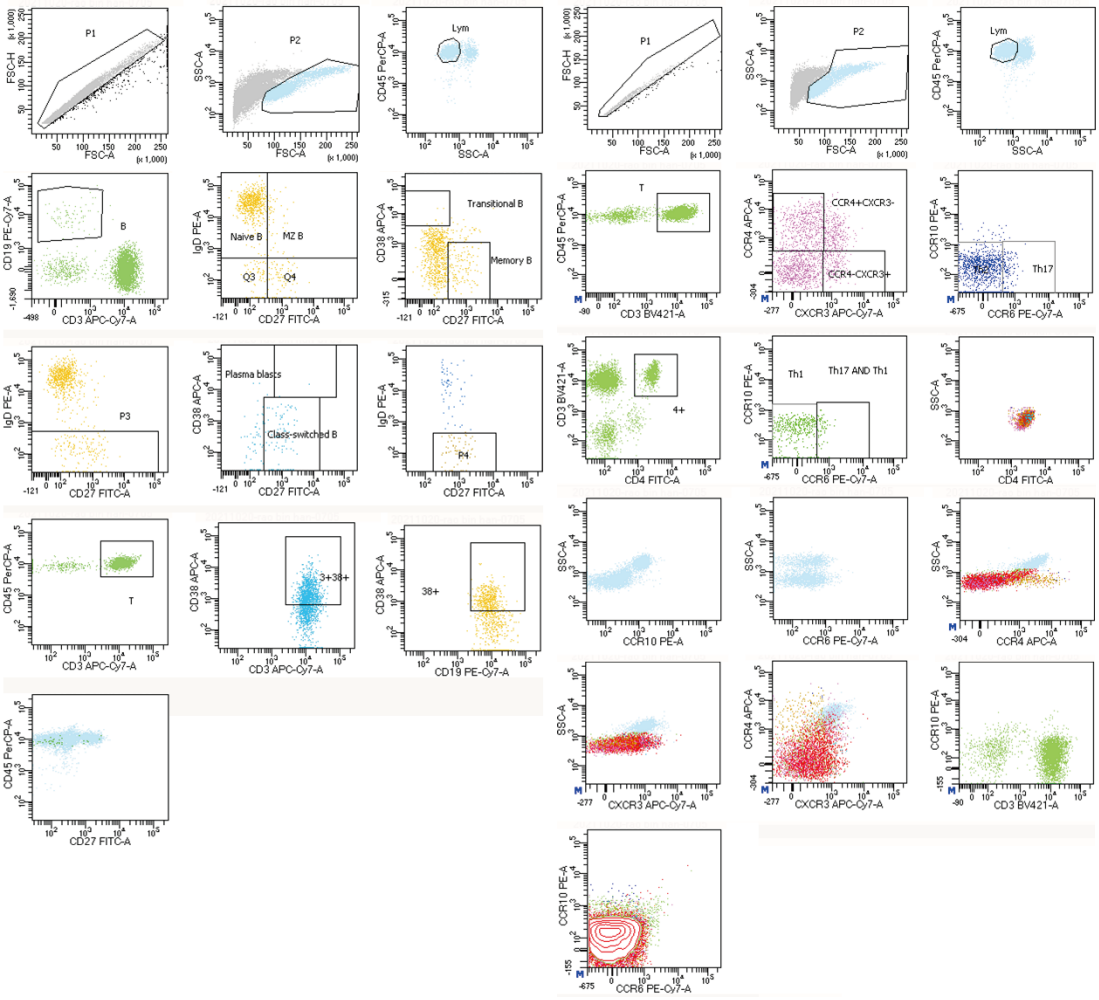

Figure S22 | Flow cytometry analysis of B cell and Th cell subsets in N3.

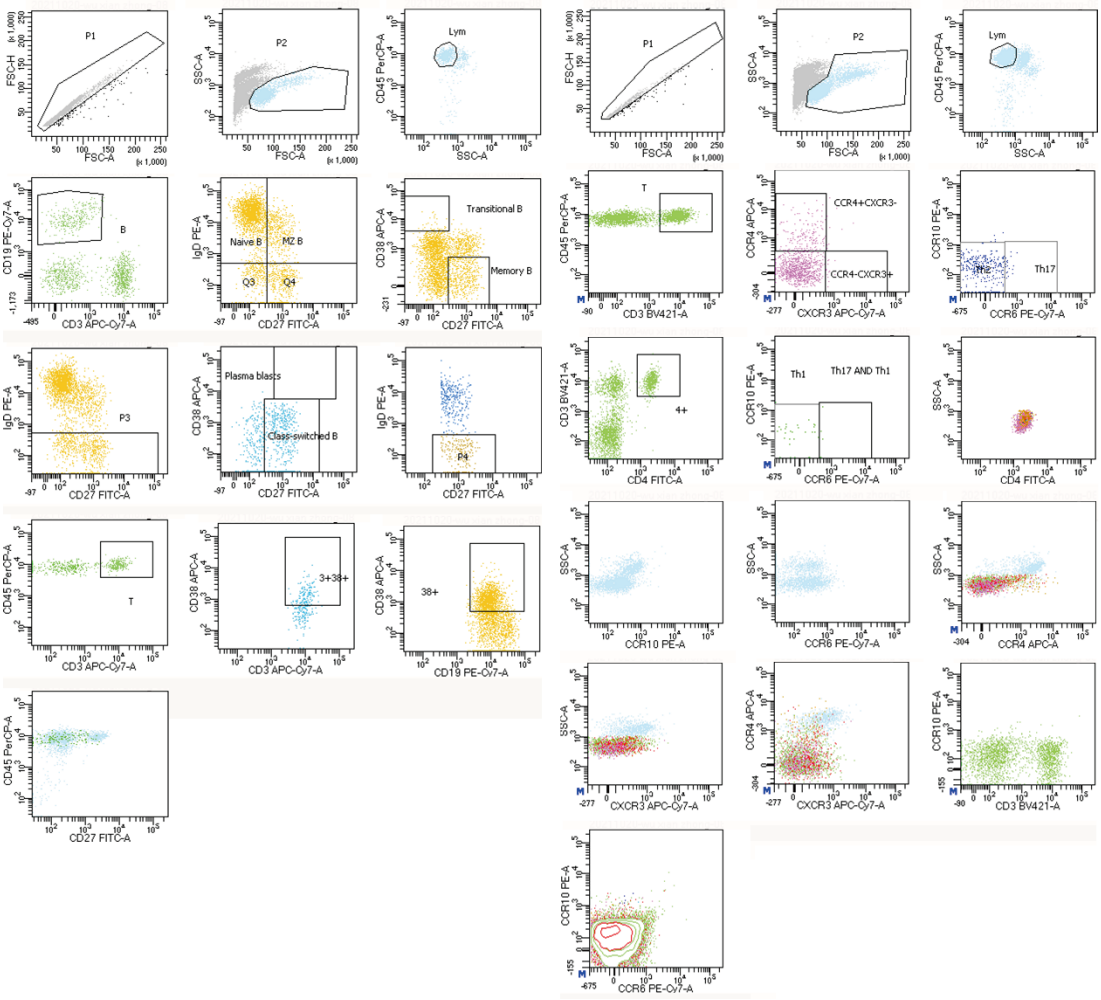

Figure S23 | Flow cytometry analysis of B cell and Th cell subsets in N4.

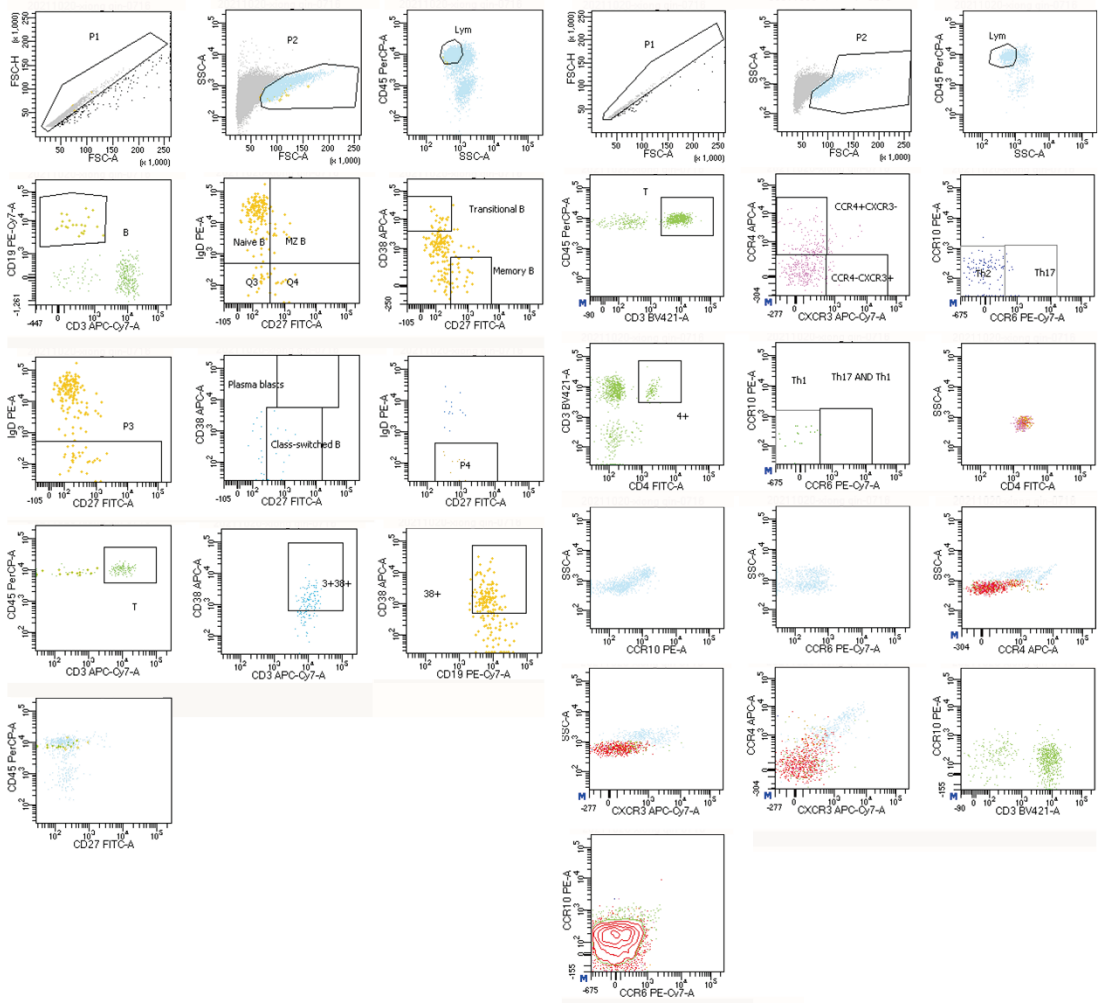

Figure S24 | Flow cytometry analysis of B cell and Th cell subsets in N5.

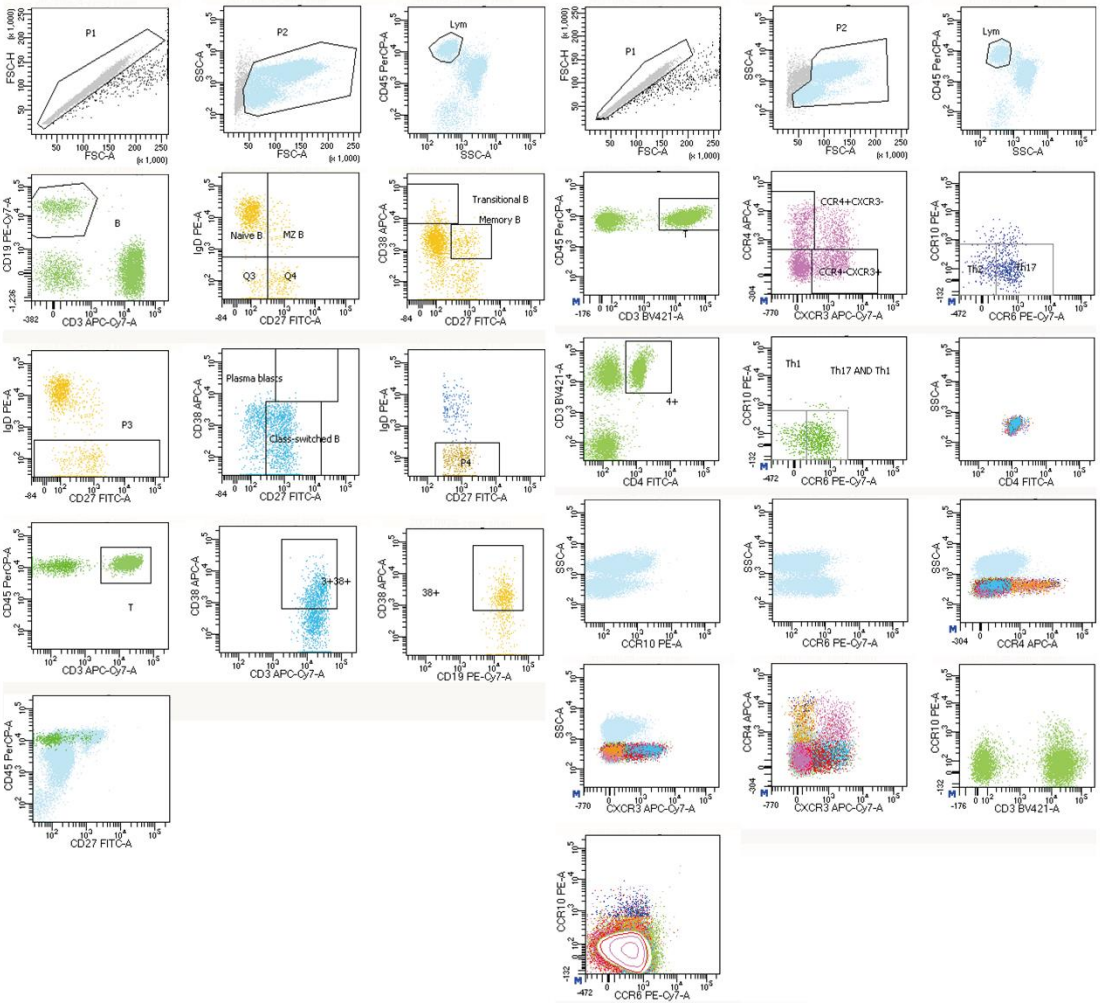

Figure S25 | Flow cytometry analysis of B cell and Th cell subsets in H1.

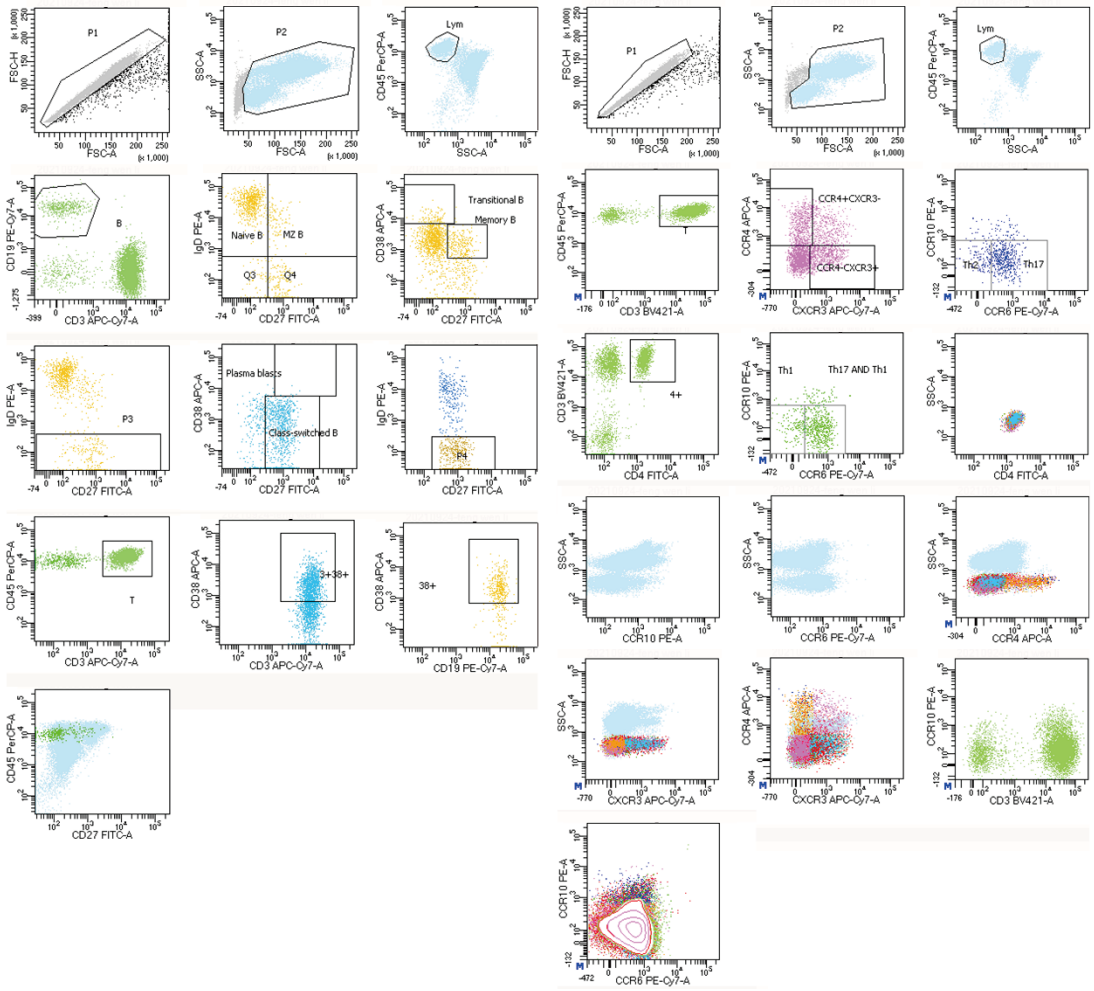

Figure S26 | Flow cytometry analysis of B cell and Th cell subsets in H2.

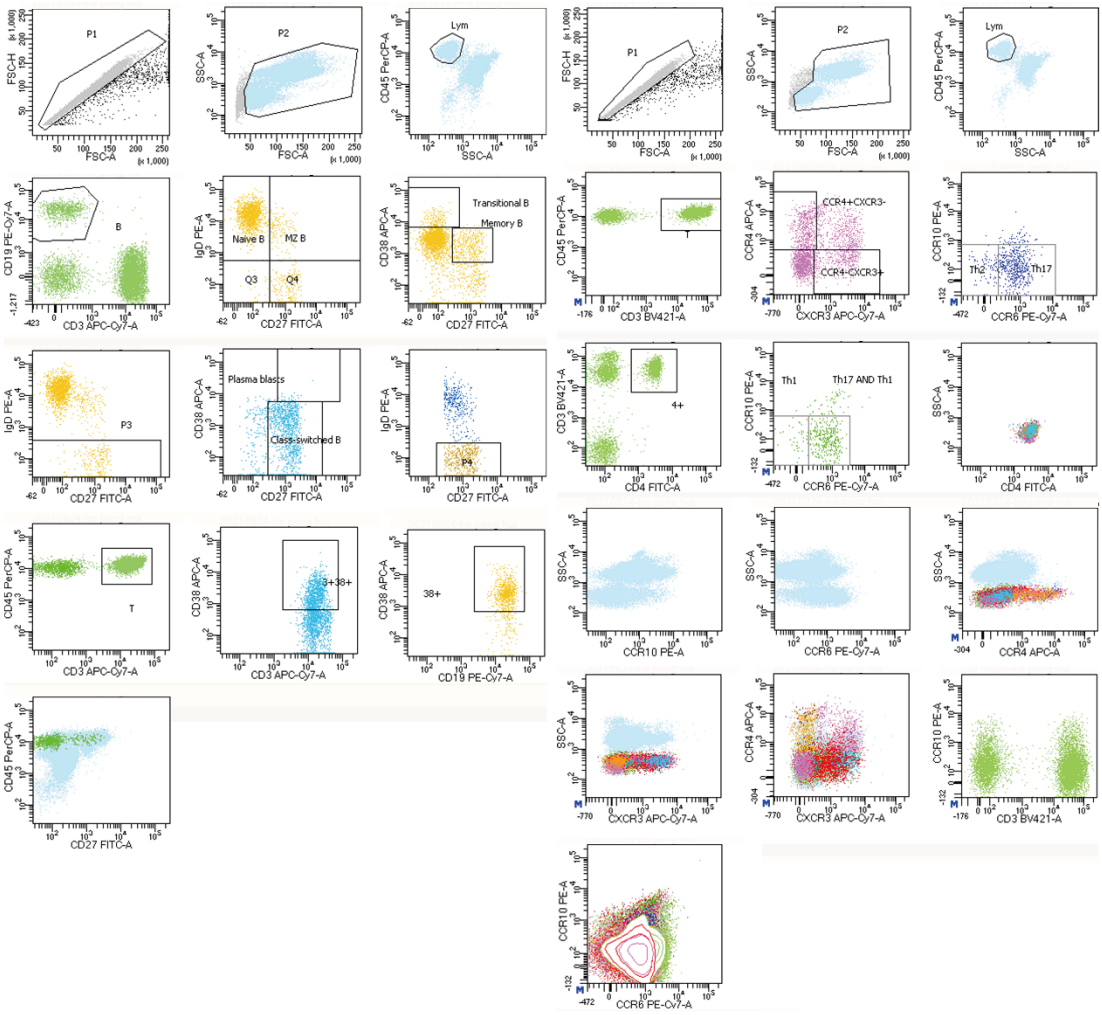

Figure S27 | Flow cytometry analysis of B cell and Th cell subsets in H3.

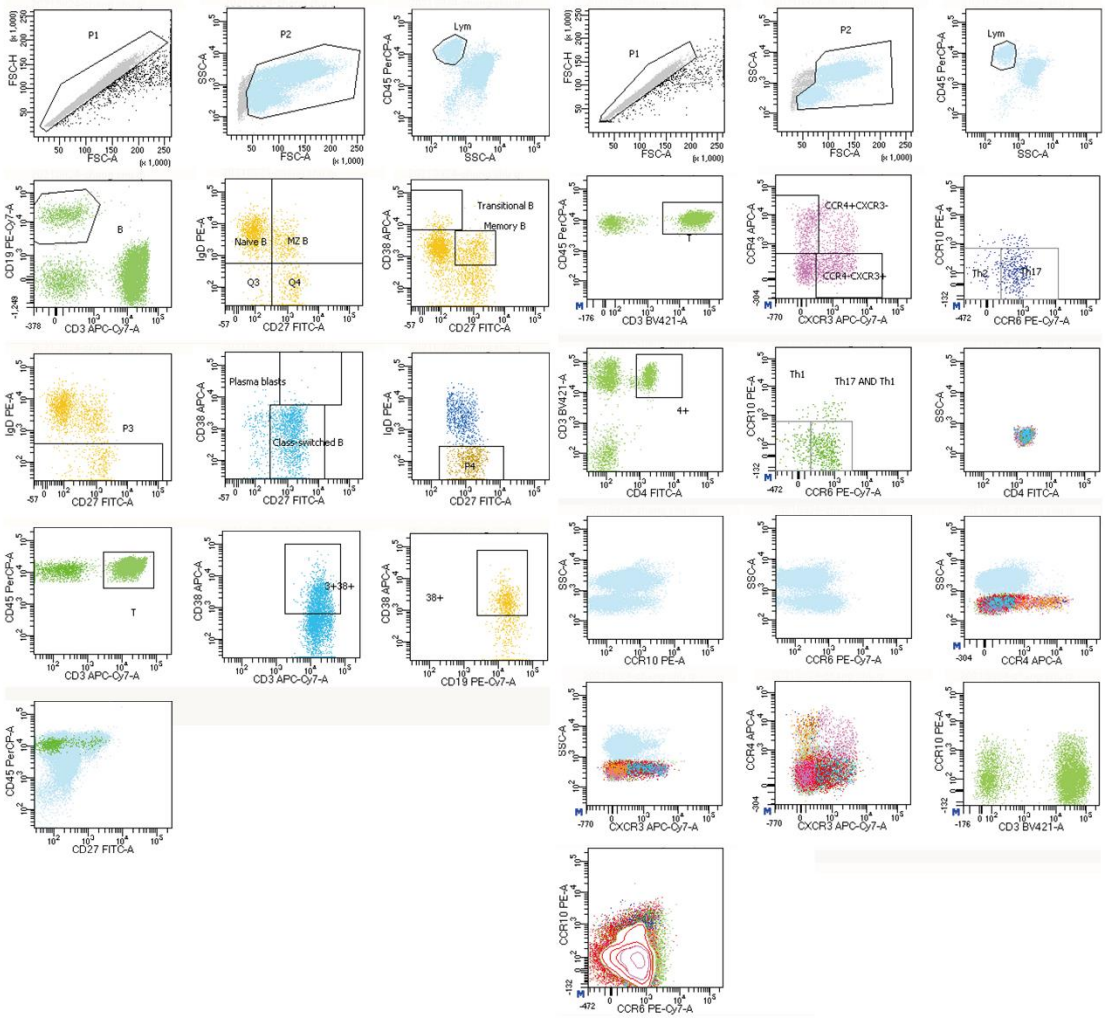

Figure S28 | Flow cytometry analysis of B cell and Th cell subsets in H4.

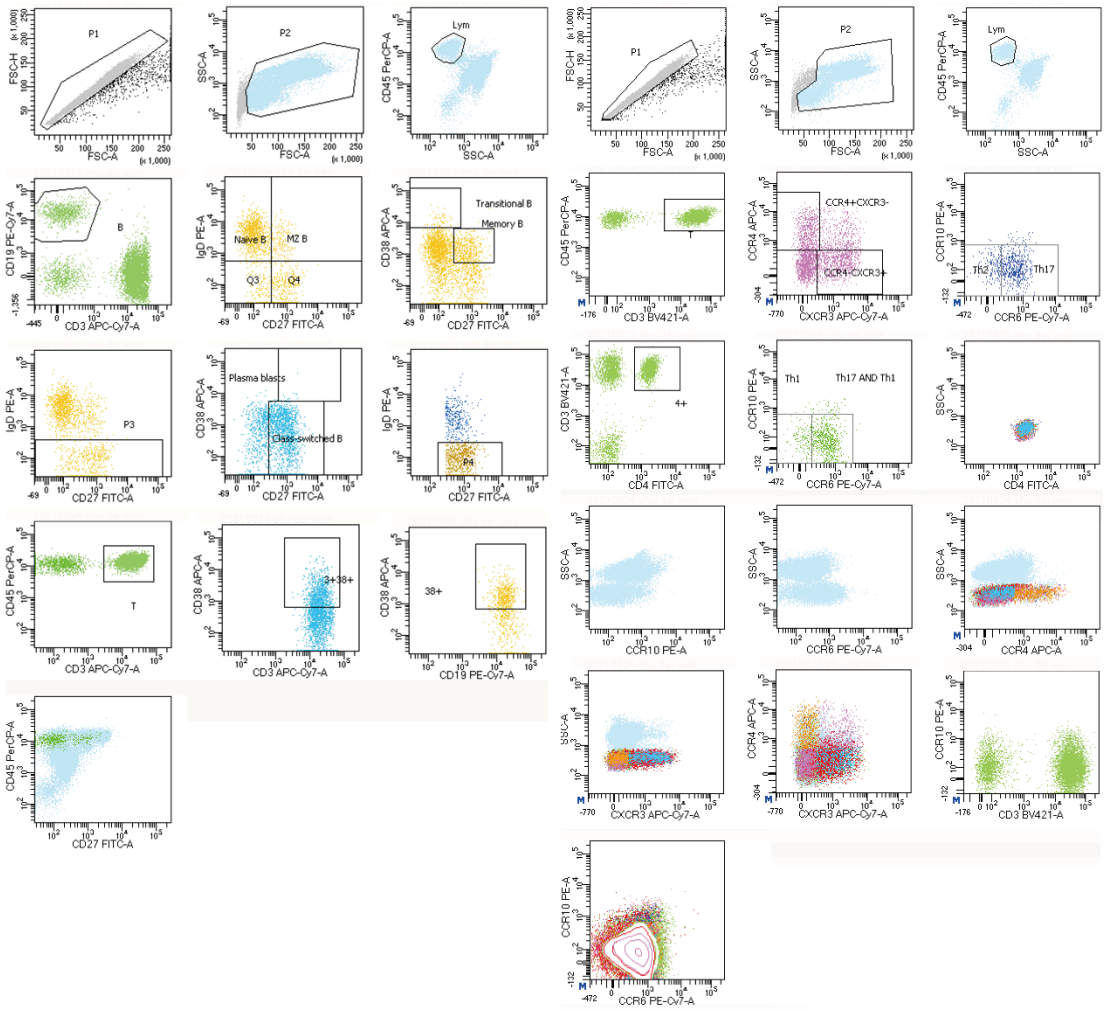

Figure S29 | Flow cytometry analysis of B cell and Th cell subsets in H5.

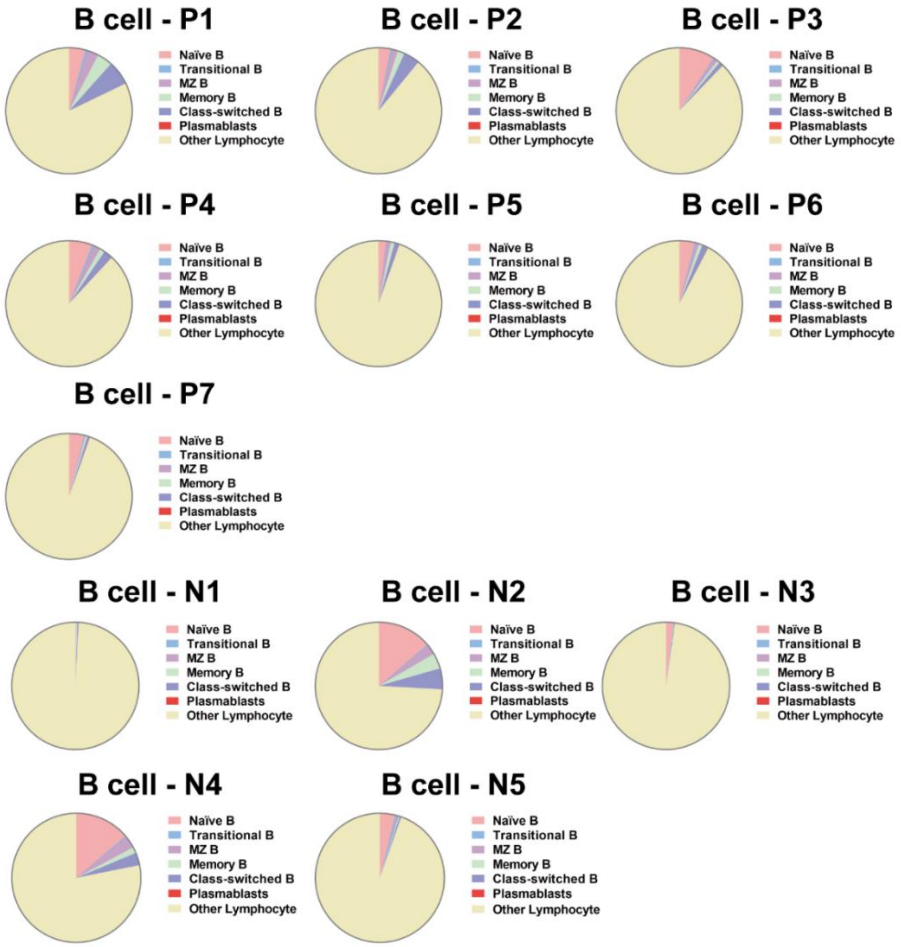

Figure S30 | The B cell subsets distribution in lymphocytes of seven IgG^{+}/IgM^{+} KTRs (P1-P7) and five IgG^{-}/IgM^{-} KTRs (N1-N5).

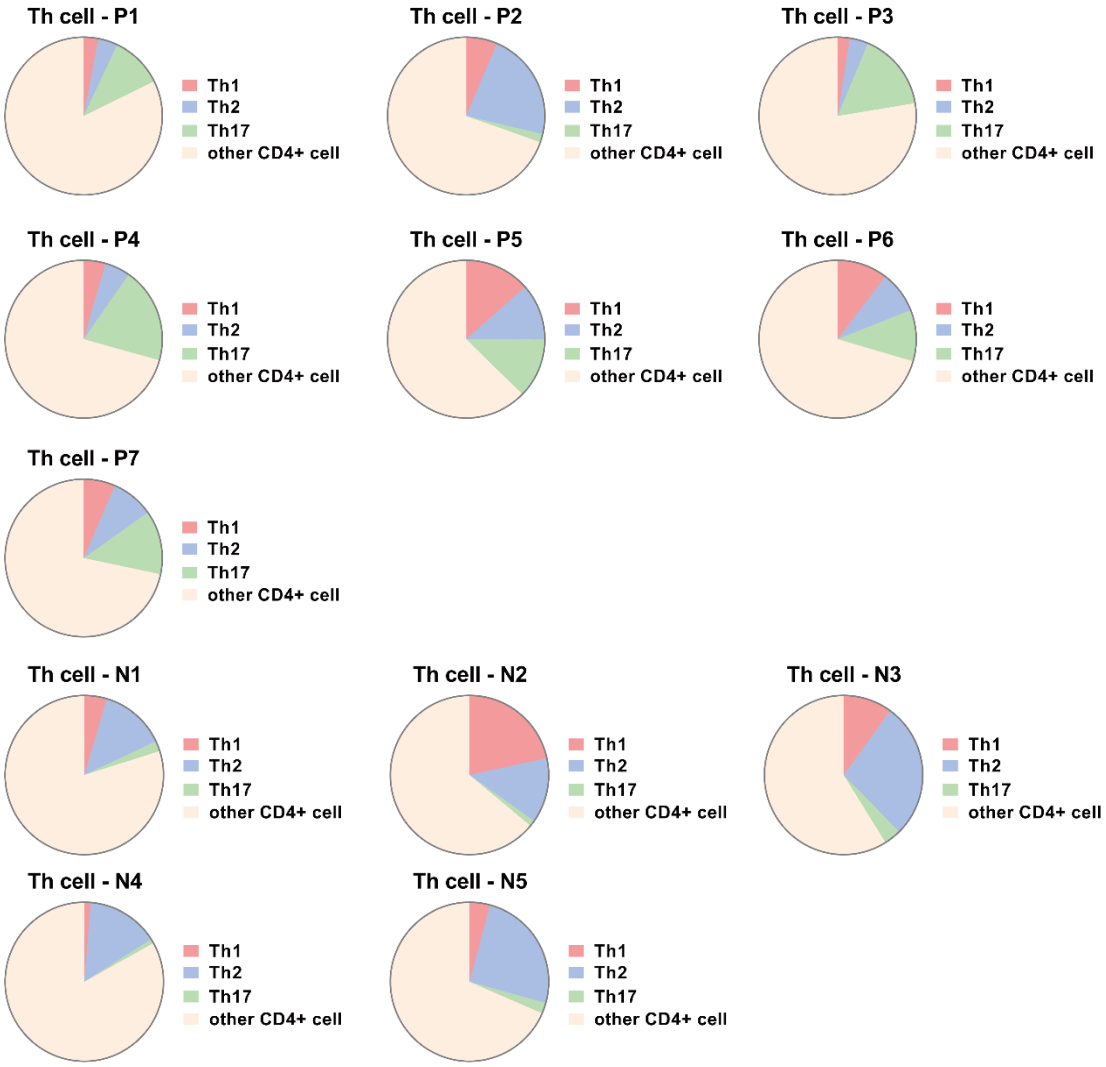

Figure S31 | The Th cell subsets distribution in $CD4^+$ cells of seven IgG^+/IgM^+ KTRs (P1-P7) and five IgG^-/IgM^- KTRs (N1-N5).

Table S4. The description and phenotypes of investigated B cell subtypes and the medians with minimum and maximum of proportional in two KTR cohorts.

Description	Phenotype	Denominator	Proportional (%) Median (Range)	
			Cohort 1 (IgG^+/IgM^+)	Cohort 2 (IgG^-/IgM^-)
Lymphocyte	$CD45^+$ SS (low) FS (low)	White Blood Cells	16.6 (11.6-55.6)	79.8 (72.9-94.4)
T cells	$CD3^+$	Lymphocytes	68 (50.2-86.2)	75.7 (42.1-84.2)
B cells	$CD19^+$ $CD3^-$	Lymphocytes	11 (4.9-14.3)	5 (0.9-22.4)
Naive B cells	$CD19^+$ $CD27^-$ IgD^+	B cells	54.6 (26.0-78.7)	63.6 (21.0-78.4)
Transitional B cells	$CD19^+$ $CD27^-$ $CD38^{high}$ IgM^+ $CD24^+$	B cells	2.9 (1.7-4.1)	1.4 (0.8-11.2)
MZ B cells	$CD19^+$ $CD27^+$ IgD^+	B cells	13.5 (5.5-23.8)	7.3 (1.2-14.1)
Memory B cells	$CD19^+$ $CD27^+$ $CD38^{dim}$	B cells	13.7 (6.2-27.7)	7.1 (5.0-32.1)
Class-switched B cells	$CD19^+$ $CD27^+$ $CD38^{dim}$ IgD^- IgM^-	B cells	23.6 (9.1-43.3)	14.5 (7.8-32.1)
Plasmablasts	$CD19^+$ $CD27^{high}$ $CD38^{high}$ IgD^- IgM^-	B cells	0.5 (0.2-1.1)	0.1 (0.0-1.2)
Th1	$CD3^+$ $CD4^+$ $CCR4^-$ $CXCR3^+$ $CCR6^+$	$CD4^+$ cells	6.4 (2.5-13.5)	4.6 (1.3-21.6)
Th2	$CD3^+$ $CD4^+$ $CCR4^+$ $CXCR3^-$ $CCR6^-$	$CD4^+$ cells	8.6 (3.8-22.3)	14.7 (13.2-27.6)
Th17	$CD3^+$ $CD4^+$ $CCR4^+$ $CXCR3^-$ $CCR6^+$ $CCR10^-$	$CD4^+$ cells	12.2 (1.7-19.6)	2.1 (0.9-3.5)

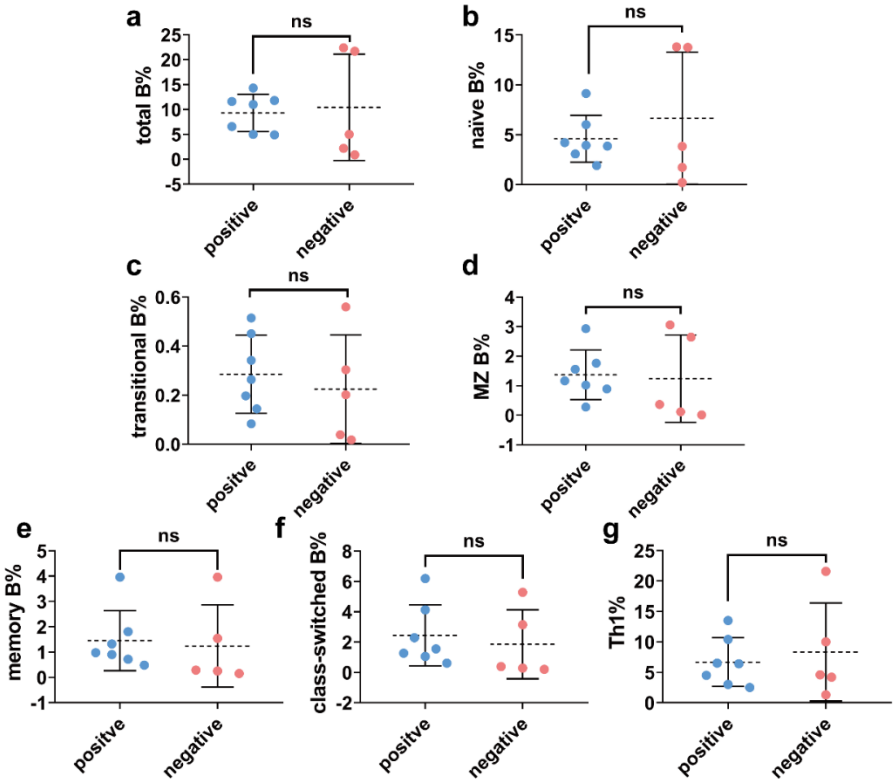

Figure S32 | Anti-RBD positive *v.s.* negative KTRs. (**a-f**) The percentage composition of total B cell (**a**, p = 0.9506) and five B cell subsets: naïve B (**b**, p = 0.6570), transitional B (**c**, p = 0.8696), marginal zone (MZ) B (**d**, p = 0.9711), memory B (**e**, p = 0.9482) and class-switched B (**f**, p = 0. 8497) in lymphocyte of seven IgG^+/IgM^+ KTRs and five IgG^-/IgM^- KTRs. Unpaired t-tests showed no statistically significant differences of these variables between the two cohorts ($p > 0.05$). (**g**) The percentage compositive of Th1 in $CD4^+$ cells of the seven IgG^+/IgM^+ KTRs and five IgG^-/IgM^- KTRs ($p = 0.8484$). The two cohorts had no statistically significant difference in Th1 levels.

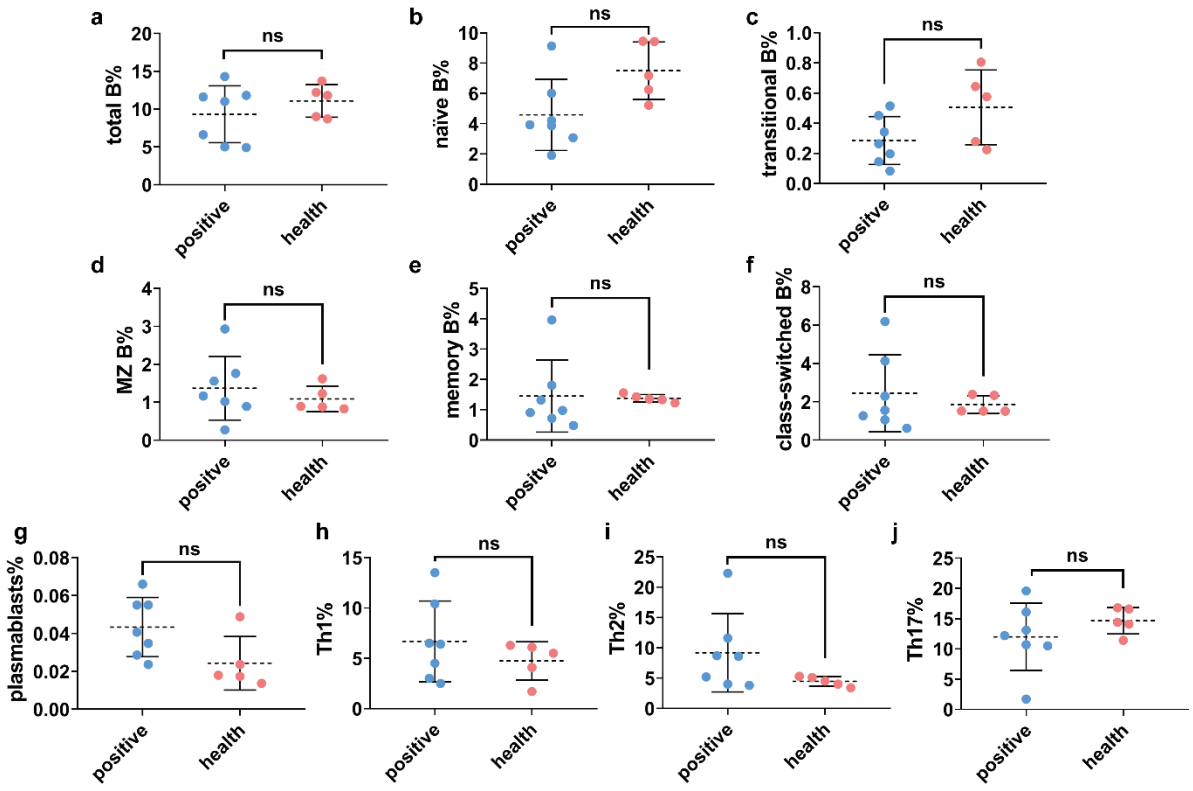

Figure S33 | Anti-RBD positive KTRs *v.s.* anti-RBD positive health participates. (**a-f**) The percentage composition of total B cell (**a**, p = 0.8835) and five B cell subsets: naïve B (**b**, p = 0.4463), transitional B (**c**, p = 0.1971), marginal zone (MZ) B (**d**, p = 0.8756), memory B (**e**, p = 0.9935), class-switched B (**f**, p = 0.8452) and plasmablasts (**g**, p = 0.0773) in lymphocyte of seven IgG^+/IgM^+ KTRs and five IgG^+/IgM^+ healthy participates. (**g**) The percentage compositive of Th1 (**h**, p = 0. 7974), Th2 (**i**, p = 0. 3559), and Th17 (**j**, p = 0. 4831) in $CD4^+$ cells of the seven IgG^+/IgM^+ KTRs and five IgG^+/IgM^+ healthy participates. Unpaired t-tests showed no statistically significant differences of these variables between the two cohorts ($p > 0.05$).